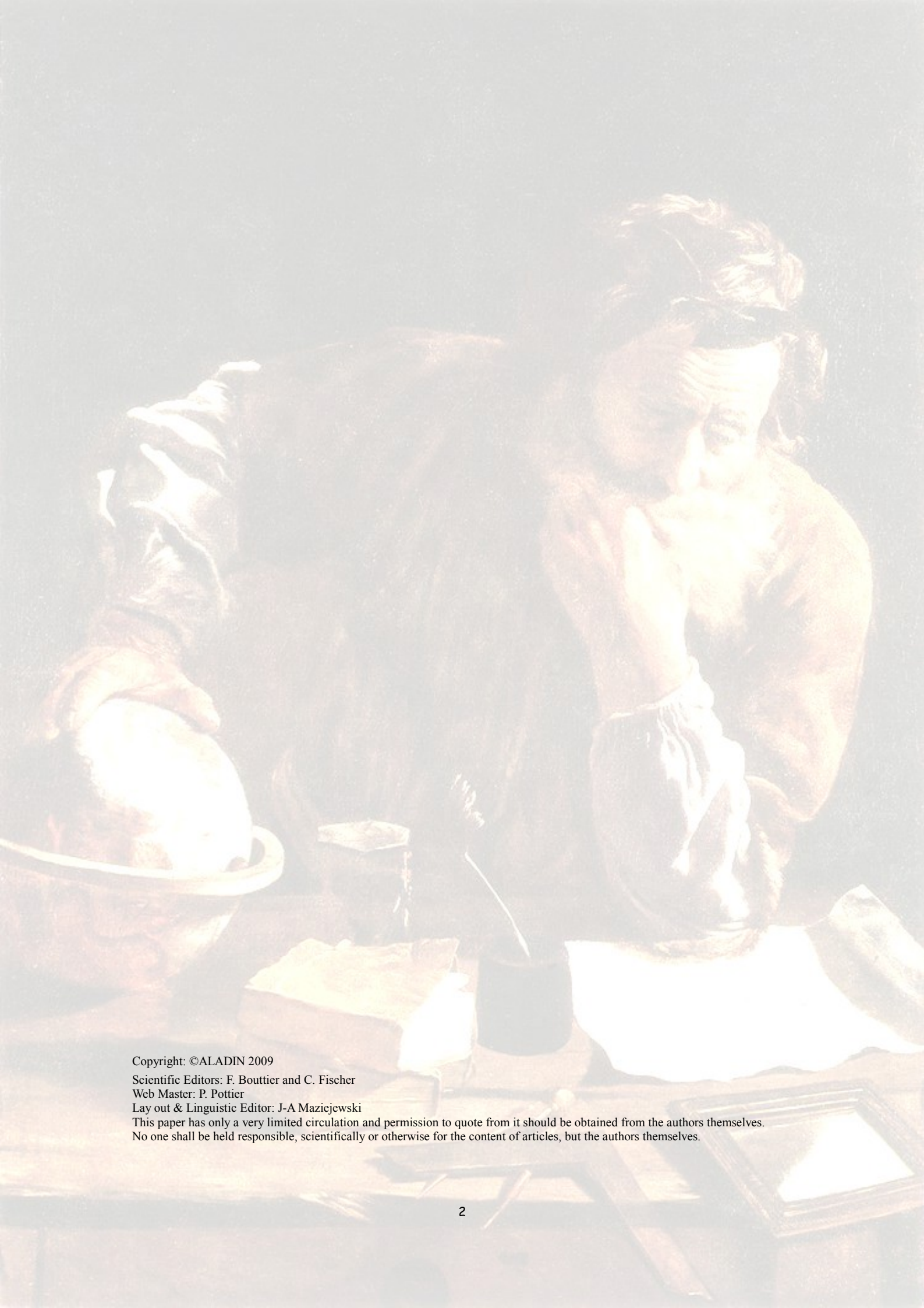




ALADIN NEWSLETTER 36

January-July 2009



Copyright: ©ALADIN 2009

Scientific Editors: F. Bouttier and C. Fischer

Web Master: P. Pottier

Lay out & Linguistic Editor: J-A Maziejewski

This paper has only a very limited circulation and permission to quote from it should be obtained from the authors themselves.

No one shall be held responsible, scientifically or otherwise for the content of articles, but the authors themselves.

CONTENT

1.FOREWORD	4
2.ANNOUNCEMENTS	6
3.OPERATIONS	7
3.1.CYCLES.....	7
3.2.CROATIA.....	12
3.3.POLAND.....	13
3.4.ROMANIA.....	14
3.5.SLOVAKIA.....	16
4.RESEARCH & DEVELOPMENTS	17
4.1.ROMANIA.....	17
4.2.SLOVAKIA.....	22
5.PAPERS and ARTICLES	24
5.1. <u>The application of the Ensemble Transform Kalman Filter technique in the ALADIN 3D-VAR system in Hungary</u>	24
5.2. <u>Forecasting Tropical Cyclones using ALADIN</u>	33
5.3. <u>Evaluation from large-scale to meso-scale simulated rainfall in regard to October 2008 observations</u>	39
5.4. <u>Ensemble background-error variances: Objectives Filtering and Impact Studies</u>	47
5.5. <u>Monitoring the coupling update frequency on the LACE coupling domain</u>	50

1. FOREWORD

Dear reader,

Times are changing. The boundaries of NWP consortia and model communities are fuzzy as ever: the last (and excellent) Aladin workshop in Utrecht has been so well integrated with the Hirlam All Staff Meeting, that it has become hard to tell them apart. The LACE acronym is popping up in new and unexpected places, the ALADIN and HIRLAM models seem to be endangered species, whereas no-one seems quite sure what HARMONIE is... or is not.

But names probably do not matter. The important is to provide the best forecasts we can, so we need to focus on the user objectives: realistic precipitation forecasts. Appropriate warnings of severe convection and wind-storms, avoiding false alarms and undetected events. Accurate low-level parameters. Progress in responding to new demands such as fog forecasts, warnings of road icing or tornado risk, improved services to the aviation sector. Our users do not care too much about our model nicknames, but they do notice when competing weather centres do a better job than us. And our taxpayers expect us to make good use of the tools they have already paid for: observing networks, radars and satellites, new supercomputers, ECMWF forecasts (in member and associated states). For instance, the IFS will soon cover Europe with excellent NWP products at 16km resolution: are we prepared to demonstrate that national models of similar resolution are indeed bringing added value ?

We need to concentrate our resources where they are most needed. Our consortium leaders rightfully complain that we should put more staff on top priority topics. Consortium-level priorities may not be exactly compatible with national ones, but we would probably all benefit from a better consistency between the work plans, and the actual staffing on the various R&D topics. It is not an easy goal. There is virtually no financial incentive to do that (as there is in e.g. European contracts). We still need to improve our practices so that working with a distant colleague should be nearly as pleasant and efficient as with a local one. Some progress has recently been made with HIRLAM about common code management. I believe we should keep improving our web collaboration tools and teleconferencing facilities in order to foster informal everyday collaboration, and to reduce the environmental footprint of our international meetings. One could imagine better shared experimental facilities too, which means solving issues of portability across computing centres, and despite scientific differences in local implementations - a result obtained in one NWP system may or may not be valid in another one that uses different scientific options.

Clearly, aiming to show to our national bosses, that we do something unique to serve each of them best, can sometimes hurt the effectiveness of international cooperation. And we may be so overwhelmed by local duties that we are not doing enough international networking. The motivation to improve may well come from the outside, as new challenges, that exceed the capabilities of our national services, may force us to work in a more distributed way, e.g.:

common IFS/ALADIN/HIRLAM code management has been a manageable problem until now, but it may require a new organization as HIRLAM increases its activities on the HARMONIE joint software;

central scientific problems such as grid-scale convection and the scale-dependency of precipitation forecasts seem to be understaffed. Perhaps they might not be solved until we make a bigger investment to understand and overcome them. They seem too complex to be solved by casual part-time studies: we may need to train and dedicate full-time experts on them. Conversely,

we might get away with temporarily stopping our activities on some old-time topics that are no longer crucial to our NWP performance... or that have failed to live up to their expectations.

we need to work on the parallelisation and technical optimisation of our NWP software. This comes from the rise of new, massively parallel computer technologies. The unchecked growth of the complexity of our IFS/ALADIN common software platform may also be a problem. A huge software rewriting effort may be needed in the next few years. Although this may not be considered glamorous from a scientific point of view, inefficient software will inevitably lead to NWP configurations that are below the international state of the art. It would jeopardize both our NWP competitiveness and our ability to make interesting scientific work with it. Having a too ambitious scientific programme can be counterproductive if it means neglecting software maintenance and optimisation, which may not have received the attention it deserves in recent years. Also, revamping our NWP software to make it more user-friendly to scientists, as envisioned in ECMWF's OOPS (Object Oriented Prediction System) project may attract a new workforce.

the SRNWP "interoperability" and related programmes still have a limited scope, but their practical implications may grow. The increasing practice of coupling our LAMs to the IFS is a related phenomenon, linked to an increasing will to use ECMWF resources better. It means devoting more effort on developments that are shared between many national teams and thus require transversal management.

François Bouttier

2. ANNOUNCEMENTS

[31st EWGLAM & 16th SRNWP joined meetings, 28/09-1/10/2009, Athens](#)

[Bureau meeting, Brussels, October 14, 2009](#)

[SURFEX training course, Toulouse, 14-16 October 2009](#)

[Regular 14th General Assembly of ALADIN Partners, Istanbul, 12-13 November 2009](#)

3. OPERATIONS

3.1. CYCLES

3.1.1. Cycles installed at Météo-France:

□ **CY36: Start of phasing on May 5th 2009 (common with ECMWF/IFS)**

- MF and partners contributions on top of CY35T2:
 - AROME: MASDEV4.8 (mostly new EDKF scheme for shallow convection) – S. Malardel and Y. Seity –
 - HIRLAM: shallow convection code from KNMI (W. De Rooy) via Sylvie+Yann's contribution (routines moved to “arp/phys_dmn” and renamed)
 - cleanings in the SL code, especially some reorganization of the SL/AD code (K. Yessad)
 - updated code in the dynamics for rotated/tilted Mercator, including both direct, TL and AD versions (P. Bénard, J.-D. Gril, G. Kerdraon, F. Vaña)
 - some small rearrangement of the code for spectral orography filtering under key LSPSMORO in e923 (M. Dahlbom, F. Taillefer)
 - minor bugfixes: SPECTRAL_FIELDS, SUEJBBAL (O. Vignes)
 - introduction in MF’s “bator” of the facility to read the BUFR format version from an external file (rather than an “IF” statement in the code). This facility will be first tested for IASI data in ECMWF’s BUFR version by Hirlam (D. Puech, F. Guillaume, R. Randriamampianina)

CY36 has been declared in July 2009.

□ **CY36T1: to be prepared over November/December; deadline for contributions about mid/end-October 2009**

- Assimilation:
 - Cleaning of Neural Network routines for AIRS (V. Guidard)
 - Microwave radiances:
 - Addition of emissivity parameterization using a Lambertian approximation for refractivity (F. Karbou) and compare with the specular hypothesis,
 - add the term emissivity*Tsurf ($\epsilon.T_s$) to the control vector as a new sink variable for VarBC (E. Gérard & F. Karbou),
 - assess surface emissivity over sea and land ice
 - assess the dynamical emissivity retrievals obtained with MERIS channels
 - infrared radiances:
 - Computation of cloud top pressures for cloudy IASI radiances (performed once during screening with a different formulation than in the IFS, V. Guidard and N. Fourrié). Same development already is operational for AIRS.
 - Extension of the MSG/SEVIRI raw radiance assimilation in the LAMs (Aladin and Arome) to cloudy radiances (S. Guedj)
 - Adaptation of code to use the ECMWF bias correction for radiosonde and SYNOP at Météo-France (P. Moll)
 - preparation for the pre-treatment of ADM/Aeolus data at MF, mostly in the “bator” pre-processing tool (C. Payan, C. Desportes) – to be confirmed
 - bugfix for the correct check of observation positions for big LAM domains in rotated geometry (OBATABS) (J.-D. Gril)
- Model dynamics:

- Miscellaneous cleanings following the agreements between MF+partners and ECMWF, based on Karim's document

- Arpège/Aladin-France physics:

- Finalize the code for using the external surface scheme SURFEX
- Plug-in for using EDKF; tunings for vertical turbulence (TKE-CBR) and shallow convection KFB

- Adaptations for using 3MT (modular multi-scale microphysics/turbulence) – J.-M. Piriou

- Cleaning of the MF_PHYS interface (reduce substantially the number of dummy arguments) – Y. Bouteloup

- Add tendencies from the dynamics to the DDH diagnostic package (F. Voitus)

- Arome:

- Protection against negative values in the turbulence scheme
- New diagnostic fields for wind gust (max value over the last 10 mns)
- Introduction of SURFEX Version 5
- Proper patch to take into account gridpoint Q_l and Q_i when converting T back to T_v in the minimization (case LSPRT=.T.); various other corrections for Arome/FGAT

- Alaro physics:

- Hirlam/Harmonie:

- Implementation of code to allow to run the MF+partners' physics on a different grid than the dynamics (inspired from the IFS development) (M. Hortal and A. Fitch) – to be confirmed

- Implementation of the variable map factor formulation for the LAM models, in the LAM Semi-Implicit code (based on an approximated development and inspired from the global solution already present in IFS/Arpège) (M. Hortal) – to be confirmed -

- Miscellaneous:

- Improvements in configuration 901 (CPREP1) for surface field conversion TESSEL => ISBA/SURFEX (J. Ferreira, F. Bouyssel)

- Code reorganization under POS (K. Yessad)

- Plug-in the missing model code for running the 1D vertical model version in Arpège/Aladin, "Single Column Unified Model" (??)

CY36T2: proposed deadline for contributions by end of February 2010, to be constructed in March ?

- Assimilation:

- Infrared radiances: Introduction of an alternative cloud detection method for AIRS and IASI (MMR code from Thomas Auligné), unless similar work planned at ECMWF (V. Guidard or N. Fourrié) – to be confirmed

- Arpège simplified physics schemes (O. Rivière):

- Modified gravity wave drag scheme (by ignoring the perturbations of some terms)

- New large scale precipitation scheme: adjustment Smith scheme ($Q_v \Rightarrow Q_v^*$, Q_l^* , Q_i^* , cloud fraction) followed by auto-conversion and precipitation of all condensed excess (Q_r^*)

- Convection scheme based on a simplified Betts-Miller scheme

Further code contributions until CY37 will concern:

- A thorough overhaul of the SURFEX to atmospheric models interface, in order to improve its robustness and prepare for further optimizations (make it Open-MP proof)

- An overhaul of the physics/dynamics interface (CPTEND, CPUTQY) in collaboration with the Aladin/ALARO partners

□ **CY37: so far, the proposal is for May/June 2010 (to be confirmed with ECMWF)**

Progress and plans at Météo-France:

Progress in 2008:

I. ARPEGE and ALADIN-France E-suite number 2 for 2008 (autumn/winter 2008):

- a)CY33T1
- b)assimilation of METOP/GRAS radio-occultation (as soon as regular data dissemination from provider has started),
- c)assimilation of EARS/ASCAT data
- d)more microwave radiances over land,
- e)ARPEGE physical parameterization:
- f)horizontal diffusion coefficients now similar for vorticity, divergence and temperature,
- g)vertical turbulent diffusion scheme with prognostic turbulent kinetic energy following Cuxart, Bougeault and Redelsperger (2000),
- h)shallow convection scheme from Bechtold et al. (2001), modified to provide a new source term of turbulent kinetic energy
- i)These changes lead to adjust parameters from other schemes, in particular within the extended Bougeault deep convection scheme. Furthermore, vertical diffusion, shallow convection and deep convection are somehow coupled.
- j)extend from 2 to 6 solar radiation bands in the Fouquart and Morcrette scheme,
- k)use of a version of the sea surface turbulent fluxes scheme ECUME from the GMGEC/MEMO group (see Weil et al., 2003),
- l)a scheme for improving entrainment at the top of the boundary layer (“GBM”),
- m)new Ozone monthly climatology (same as IFS),
- n)introduction of inline Fullpos post-processing
- o)ALADIN-France: same changes as ARPEGE plus introduction of the surface assimilation (CANARI) adapted from ARPEGE.

This e-suite has been switched to operations on February 4th 2009.

II. Developments preparing for the NEC 2009 upgrade, focused on a new resolution of the ARPEGE system (TL800C2.4L70) have begun end of 2008.

In the fall and winter 2008/9, a major upgrade of the production and data bases environment has entered a pre-operational and porting phase. This project has reduced the ability of the Production Department to install e-suites. As a result, it was not possible to further develop our ensemble prediction PEARP over that period. On a non-operational basis, the PEARP developers have run separately from the operational application a further 10 member group under the OLIVE framework.

AROME operational suite number 1 (spring to winter 2008):

- Forecast model configuration:
 - 600*512 gridpoint domain, 2.5 km resolution, 41 levels,
 - Méso-NH physics: turbulent kinetic energy version CBR – Cuxart, Bougeault, Redelsperger -, ICE3 microphysics that include graupel, Surfex coupled in explicit mode with atmospheric vertical diffusion including an additional CANOPY scheme for boundary layer profiles, IFS-based radiation scheme called every 15 mns, no deep

convection nor gravity wave drag,

■ timestep = 60 s *not using* the Predictor/Corrector scheme.

○ Assimilation will be with a 3 h frequency 3D-VAR cycle, including:

■ ensemble B statistics recomputed on newly tuned horizontal diffusion version of AROME

■ Arp/Ald bias correction files so far, with later on switch to VarBC

■ GPS ZTD with specific (station, center) quality control and blacklist

■ specific channel selection for AMSU data (because of different vertical discretization than ARPEGE/ALADIN-FR)

■ 10 m wind

■ 2m T and RH on daytime

■ 2m T and RH first guess values extracted from Surfex model (rather than ACHMT)

■ radar radial winds assimilated (15 km thinning)

○ 6 hourly reset to the ALADIN and ARPEGE CANARI surface.

AROME runs four times a day up to 30 h range with a 3h 3D-Var assimilation cycle. One 30h forecast currently requires about 40 minutes elapse on 56 processors on the NEC-SX8R, without post-processing.

This AROME-FR suite has been declared fit for operational use by Météo-France Forecasters on December 18th, 2008.

□ **Plans for 2009:**

• Introduce the ARPEGE ensemble-based flow-dependent □ b information in regional assimilations such as ALADIN-France, ALADIN-Réunion and possibly AROME, and prepare the installation of the ensemble assimilation for the ALADIN-Réunion system (*to be confirmed*)

• Complete Acceptance Test ("VSR" in French acronym) of NEC Phase 2 upgrade: completed on week 25 (June).

• The operational suite will be moved to the new system within 2 months after the satisfactory conclusion of the "VSR". This move shall occur asap after mid-August. It will be followed by a one-to two week shut down of the old SX8 clusters, in order to re-assemble them into one single cluster.

• ARPEGE and ALADIN-France E-suite number 1 for 2009 (summer/autumn):

○ CY35T2

○ new change of resolution of ARPEGE: T800C2.4L70

○ new resolution for the 4D-VAR analysis increment: between T340L70 and T400L70

○ move to 3 outer loops and minimizations

○ changes in the assimilation ensemble: L70

○ Double the density of about all radiance types (change the scale of data use from one spot every 250 km to one every 125 km), with a higher priority put on IASI

○ assimilation of NOAA-19 channels

○ monitoring of SSMI/S data

○ extend the number of assimilated advanced IR sensor channels (IASI, AIRS), in particular above clouds,

○ introduce a bias correction for MSLP and T observations (based on ECMWF practice),

○ ALADIN-France: L70, slight increase of resolution to about 7.5/8 km

• AROME-France E-suite number 1 for 2009:

○ AROME will inherit some of the ARPEGE/ALADIN changes: doubled radiance density, NOAA-19, extra IASI channels, switch to VarBC

- Assimilation of radar reflectivities
 - Increased vertical resolution (between 60 and 70 levels)
 - Activation of an upper level sponge towards the coupling model (in the forecast)
 - test new choice for B-level parallelization (made possible after correcting an old, sleeping bug in the B-level decomposition of LAM Semi-Lagrangian advection scheme)
 - new version of shallow convection (to increase the persistence of Sc clouds)
 - new version of CANOPY, using the Beljaars scheme, to improve low level winds over orography
 - ICE4 microphysics (including hail)
- PEARP Version 2: main target is an increase of PEARP members to about [30-40] + coupling with the ensemble assimilation + some physics perturbations + L65. Forecast set-up upgraded to the latest standard of the deterministic ARPEGE physical parameterization except those schemes contributing to the "modelling error" representation approach.

After moving the operational suite to the new super-computer framework, and once the 2009 configurations will be well under way, significant efforts will be dedicated to the following subjects. Those may influence the ALADIN activities:

- works to upgrade the organization and maintenance of the operational suite, with a view to improve productivity to switch a suite from OLIVE to operations
- revise, possibly in-depth, the schedule of the operational suite, with the primary objective of simplifying the 00 UTC production
- decide of a future for ALADIN-France: it may well be that ALADIN-Réunion becomes the reference ALADIN, supplemented by 2 or 3 overseas ALADIN

□ **Plans for 2010:**

One important change will occur in the Computer Centre, with the successive upgrades of the two NEC/SX9 clusters (add more CPU on each of them). This upgrade will require to shut down successively each cluster for about two weeks, and new Acceptance Tests will be done. This work should take place over February/March/April.

3.2. CROATIA

3.2.1. 3DVAR INSTALLATION IN CROATIA. Antonio Stanešić, Tomislav Kovačić, Kristian Horvath

Summary

After successful installation of CANARI we dedicated our efforts to installation of 3DVAR system. B matrix was computed by standard NMC method 100 forecast (K. Horvath). Assimilation cycle is set up with data coming form OPLACE. Verification is still ongoing.

Status, experiences and plans

Assimilation is done in experimental setup with cy32t3. Cycling is schematically shown on the bottom figure (Figure 1.). Surface analysis over land is done with CANARI using data from OPLACE (LACE preprocessed data) and SST is taken from Arpege long cut off file. Upper air analysis is done with all OPLACE data (except SEVIRI). 6 hour forecast is done with operational namelist (without DFI). Production is done in similar way except that SST comes from Arpege short cut off file.

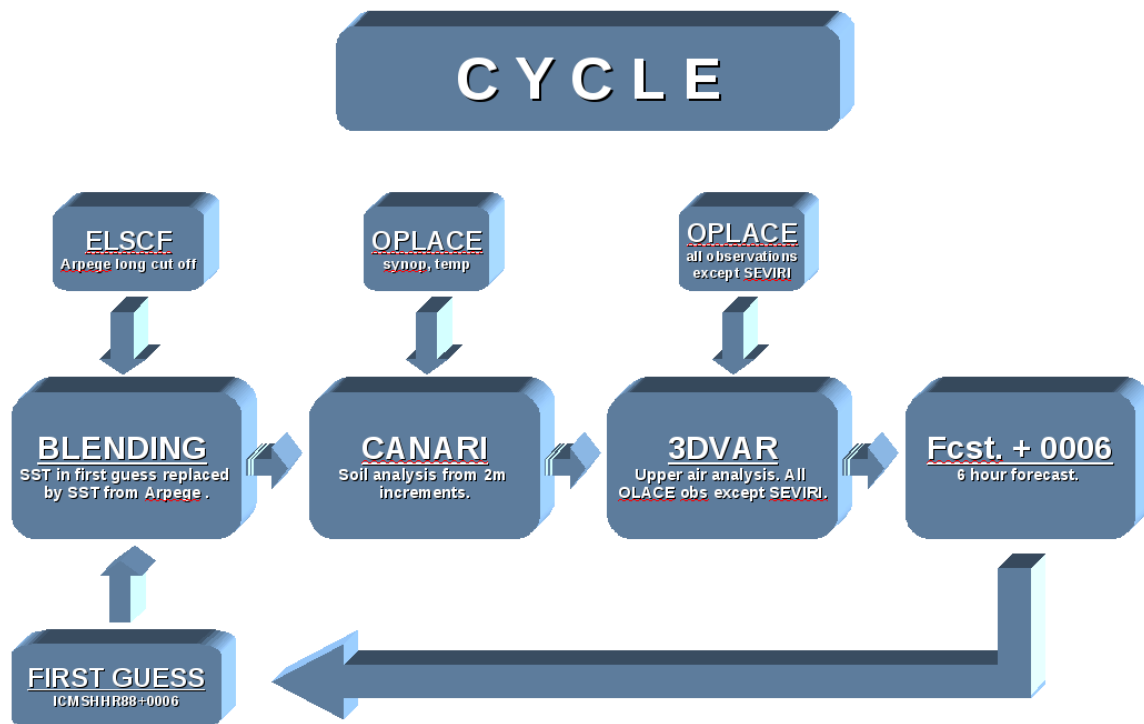


Figure 1: Schematic of assimilation cycle

Verification showed some improvement in 2m parameters (most probably due to surface analysis). Upper air statistic are not so good.

We started with impact studies of various data sets but now ongoing activities are on installation of new cycle35 (in order to test VarBC) and then we will continue with these studies.

We will also test usage of DFI in cycling (some preliminary results showed deterioration in verification scores for screen level parameters - this still has to be investigated). New B matrix will be computed with ensemble method and there is also ongoing work on verification.

Details on installation and verification of 3DVAR in Croatia can be found on poster <http://www.cnrm.meteo.fr/aladin/spip.php?action=autoriser&arg=1316>, or in report http://www.rclace.eu/File/Data_Assimilation/2008/DA_CRO.pdf.

3.3. POLAND

Marek Jerczyński (zijerczy@cyf-kr.edu.pl)

During first half of 2009 the efforts in the field of operational activities were split into 5 major tasks:

- improvement of operational software to enhance its reliability and robustness
- further development and pre operational testing of new visualization system based on NCL
- tests of ALADIN on small, 16-core linux cluster – great thanks to Jure & Jure from Slovenia for their help
- preparations to local work with AROME
- preparation of input data for INCA – cooperation with IMWM Satellite Remote Sensing Dept.

3.4. ROMANIA

3.4.1. ALADIN – ROMANIA (Doina Banciu)

Since last time there has been no changes in the operational suite, based on CY28t3.

The ALADIN model at 10 km resolution (144x144 points, 41 vertical levels) is still integrated (4 times per day) on a SUN E4500 workstation (8-CPU 400GHz, 8*1 GB RAM), using the boundary conditions from the ARPEGE model (6 hours frequency).

More recent versions of the model (CY33T1 and CY35T1) have been implemented and tested on the new available computing platform at National Meteorological Administration of Romania. It is an IBM BLADE Linux Cluster, with 14 nodes; 2 CPU-quad core/node; x86_64 processor architecture, 2.5 GHz. The operating system is “Red Hat 5.3 Enterprise”.

Tests have shown a substantial reduction of the integration time with respect to the current state.

- ◆ Using Intel Compiler:

- on the same domain, resolution, number of vertical levels and same time step (450s), using 5 nodes, the 78 hour integration time was about 15 minutes with respect to the current value of 2 hours and 40 minutes;

- increasing the number of vertical levels to 60 and reducing the time step (400 s) the integration time was 23 minutes.

N.B. For both cases the model configuration was that contained in the export model version, (i.e. containing more sophisticated radiation scheme, prognostic variables for condensed water and precipitation, etc.).

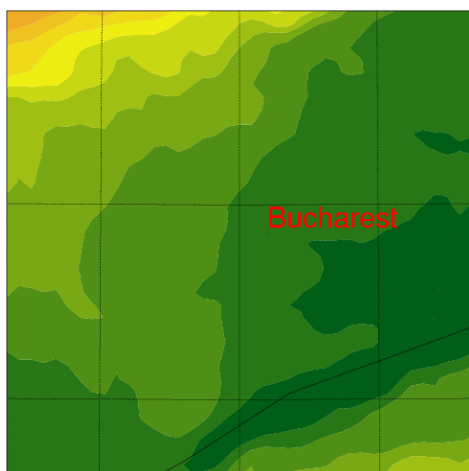
- ◆ Using Portland Compiler

- on the operational domain (144 x144 points, 41 vertical levels), using 5 node, the 24 hour ALARO integration time was about 5 minutes.

Foreseen configurations:

- ◆ ALARO: $\Delta x=10\text{km}$, 60 vertical levels, same area as present
- ◆ ALARO: $\Delta x=5\text{ km}$, 60 vertical levels, same area as present

3.4.2. ALADIN – BUCHAREST (Mihaela Caian)



- ◆ computing platform: 2CPUS SGI ALTIX 350 workstation
- ◆ domain: 50 x50 points, 41 levels, $Dx=3.5\text{ km}$
- ◆ model version: cy32t1, NH version
- ◆ the integration is followed by a dynamical adaptation ($Dx=1.5\text{ km}$)
- ◆ LBC from ALADIN Romania
- ◆ 1 run/day ; 48 h forascas range

Fig.1. Model domain and orography

The output (wind, temperature, precipitation, humidity, cloudiness, radiation) up to 48 hours is used as input to 3 pollution models: Morage, Media (at regional scale), OML (urban scale) and OSPM (street scale).

Emission data are daily updated from the Environment Agency while traffic data are yearly processed. The pollution forecast is processed in various ways for users under GIS environment and released to the mass-media on the web page of NAM, with health related recommendations provided by the Health Authority of Bucharest (Fig.2: a,b).

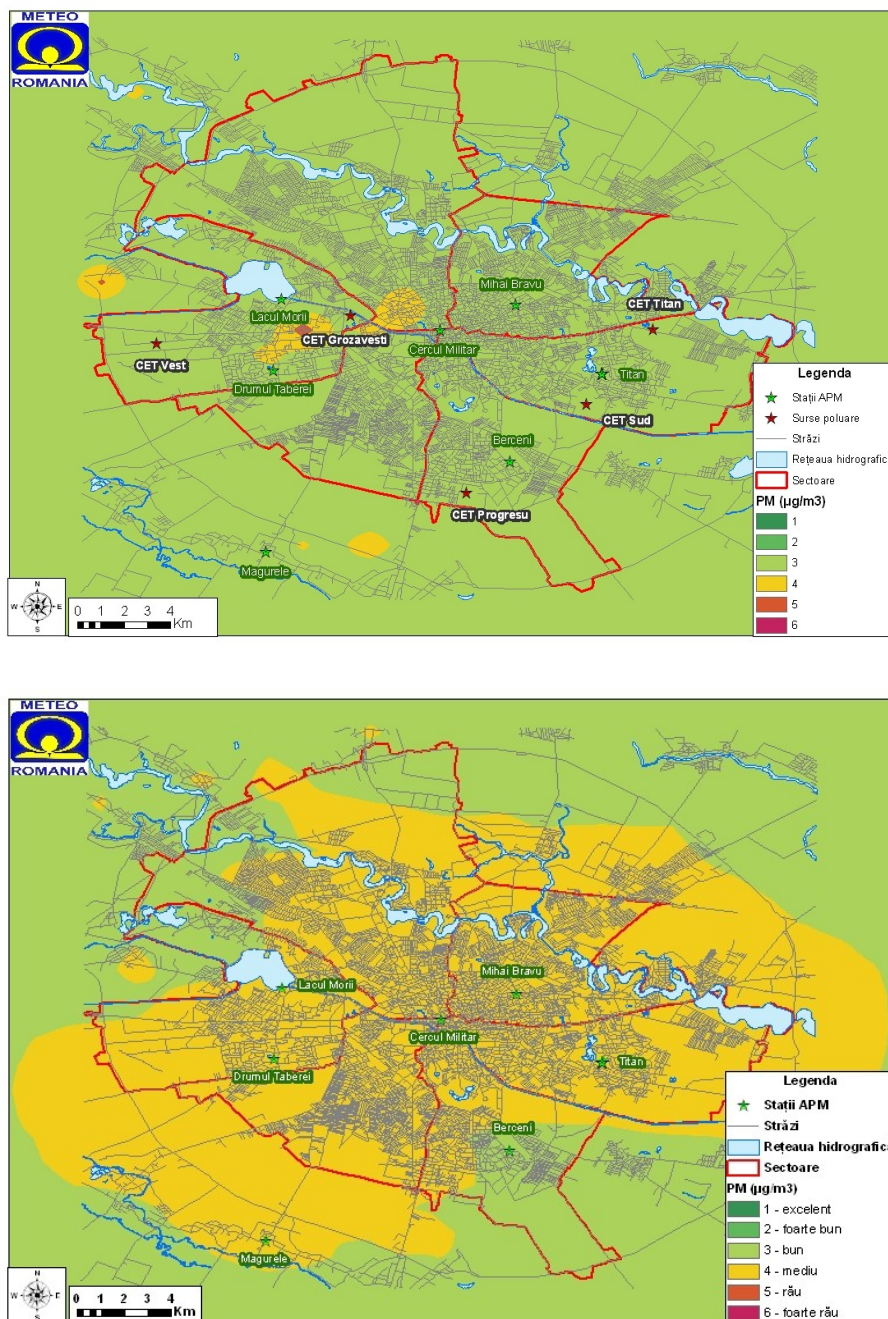


Fig.2: Air pollution forecast for PM₁₀ (average over 24 hours) the legend relates to European norms.

3.5. SLOVAKIA

3.5.1. HARDWARE

- **Computer [no change]:**
 - ◆ IBM Regatta
 - ◆ 32 CPUs of 1.7 GHz
 - ◆ 32 GB RAM
 - ◆ 1.5 TB disk array

- **Archiving facility [no change]:**
 - ◆ IBM Total Storage 3584 Tape Library with IBM Tivoli Storage Manager
 - ◆ current capacity of tapes around 30 TB
 - ◆ used for automatic backup of ICMSH files, GRIBs and selected products

3.5.2. OPERATIONAL SUITE

- **Domain and geometry [no change]:**
 - ◆ 309 x 277 points (C + I zone)
 - ◆ dx = 9.0 km
 - ◆ quadratic truncation
 - ◆ 37 vertical levels

- **Operational model version [no change]:**
 - ◆ cy32t1 - ALARO with 3MT

- **Integrations [no change]:**
 - ◆ 4 runs per day (00, 06, 12 UTC up to 72 hours, 18 UTC up to 60 hours)

- **Pseudo-assimilation cycle (Upper air spectral blending)**
 - ◆ 4 runs per day (00, 06, 12, 18 UTC up to 6 hours with long cut-off ARPEGE LBCs)
(Assimilation guess is used to copy new hydro-meteor fields, TKE and new 3MT prognostics fields)

3.5.3. ARPEGE LBC DOWNLOAD

Both assimilation and production LBC are downloaded 4 times per day. Primary channel is internet/BDPE. Backup of production LBC is done via ECMWF and ZAMG.

4. RESEARCH & DEVELOPMENTS

4.1. ROMANIA

4.1.1. Combination of ARPEGE&ECMWF EPS downscaling (S. Tascu)

The work combines ARPEGE-ECWFMF EPS developed within RC-LACE framework. The LACE verification package and bias correction method (developed at NCEP - Bo Cui, NCEP 2006) which includes two moments of adjustment were applied to the "combined" ensemble ARPEGE-IFS/ECMWF downscaled by the ALADIN model, for temperature and geopotential at 500 and 850 hPa, for July 2008. (Simona Tascu, LACE stay in Vienna, 2009).

The results show that the the bias-corrected combined ensemble and calibrated ensemble improve the short range forecast in respect with the raw combination for temperature and geopotential at 500 and 850 hPa.

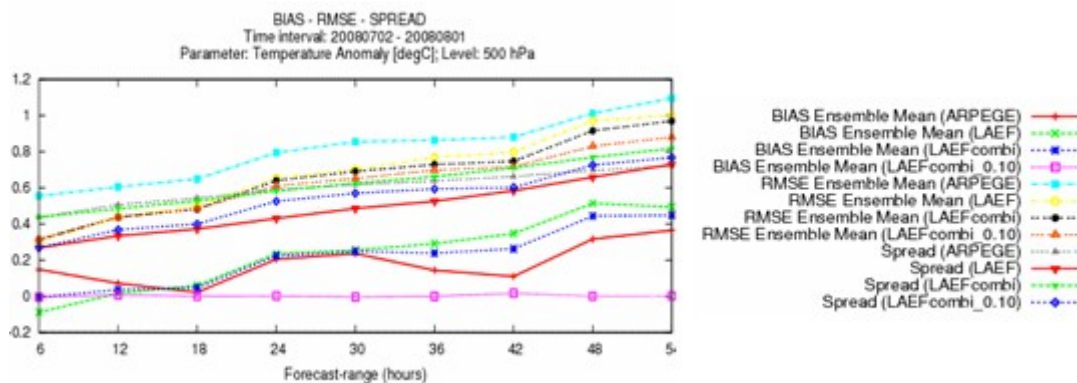


Fig.1: 500 hPa temperature Bias, RMSE and SPREAD for 3 ensembles: the raw combination (labelled LAEFcombi), the combination after 1st moment (labelled LAEFcombi_0.10_1st with 10% weight) and the combination after 2nd moment (labelled LAEFcombi_1.10_2nd).

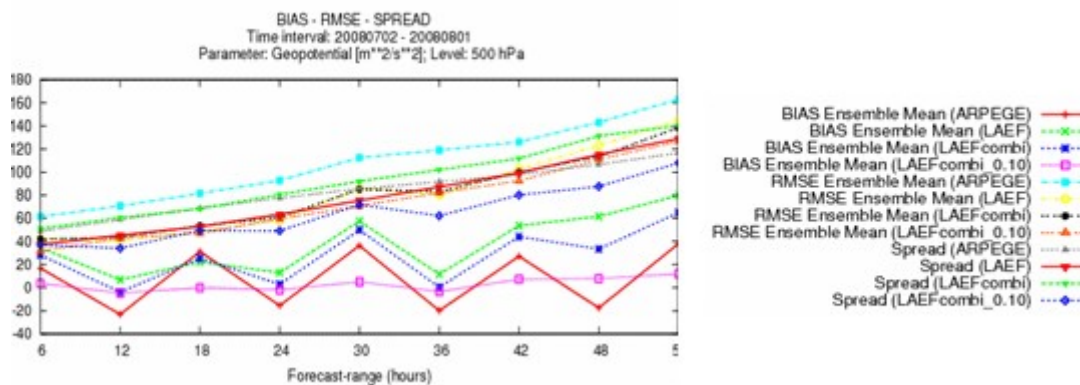


Fig.2: 500 hPa geopotential Bias, RMSE and SPREAD for 3 ensembles: the raw combination (labelled LAEFcombi), the combination after 1st moment (labelled LAEFcombi_0.10_1st with 10% weight) and the combination after 2nd moment (labelled LAEFcombi_1.10_2nd).

References

Cui, B., Toth, Z., Zhu, Y., Hou, D., Unger, D., Beauregard, S., 2006: The Trade-off in Bias Correction between Using the Latest Analysis/Modeling System with a Short, versus an Older System with a Long Archive. The First THORPEX International Science Symposium. December 6-10, 2004, Montréal, Canada, World Meteorological Organization, P281-284.

4.1.2. A Heavy precipitation case study (S. Tascu and Mihaela Caian)

For a severe weather case of high precipitation of 15 - 16 September 2008 in the eastern part of Romania (where precipitations amounted to 134 l/m² in 24 hours) the ECMWF/EPS downscaling by the Aladin model was carried out. Ten members from ECMWF/EPS (100 members of 00 and 12 runs from September 12) were selected, using the Hungarian clustering method. This method was applied for two different domains: the ALADIN coupling (120x90 points, $\Delta x = 16$ km) and integration (144x144 points, $\Delta x = 10$ km) domains used in operations. The result of the best ensemble members, obtained for the two domains of the downscaling, are shown below, in comparison with the observed precipitation and the deterministic forecast.

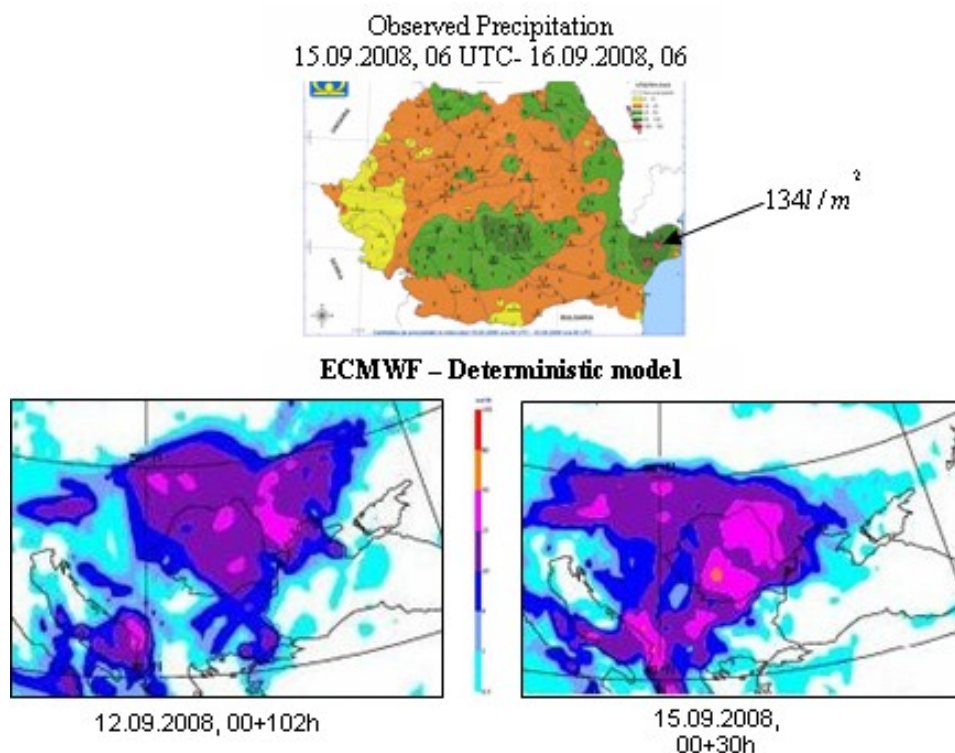


Fig.3 24 hour cumulated precipitation: 15.09.2008, 06 UTC - 16.09.2008, 06 UTC: observed-top, ECMWF forecast of 12.09.2008 00+102 h - bottom left, ECMWF forecast of 15.09.2008 00+30 h - bottom right.

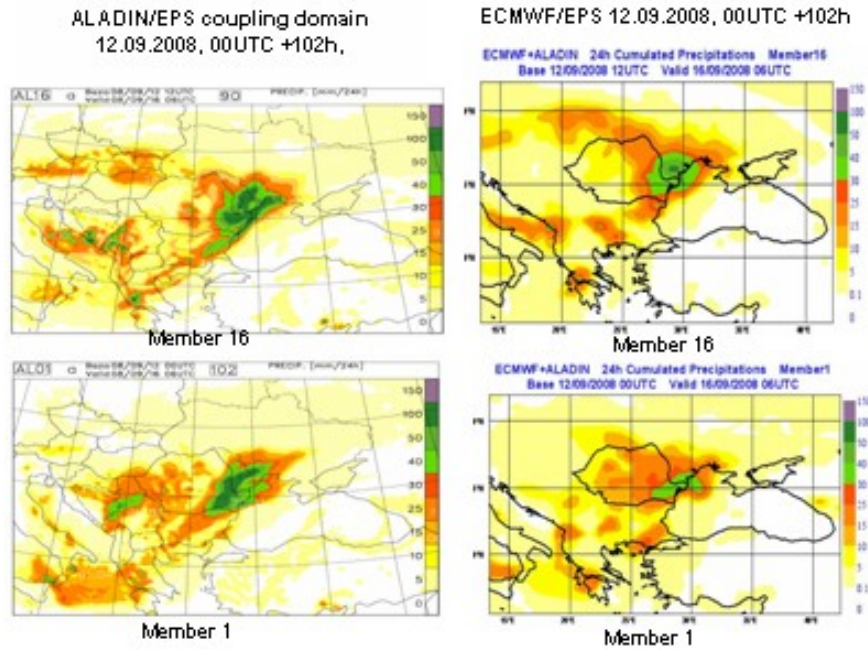


Fig.4: 24 hour cumulated precipitation:15.09.2008, 06 UTC -16.09.2008, 06 UTC for the 102 hour (started at 12.109.2008, 00 UTC) ALADIN (left) and ECMF(right) forecast integrated over the coupling domain, for the best members: 16 - first row) and 1 - second row

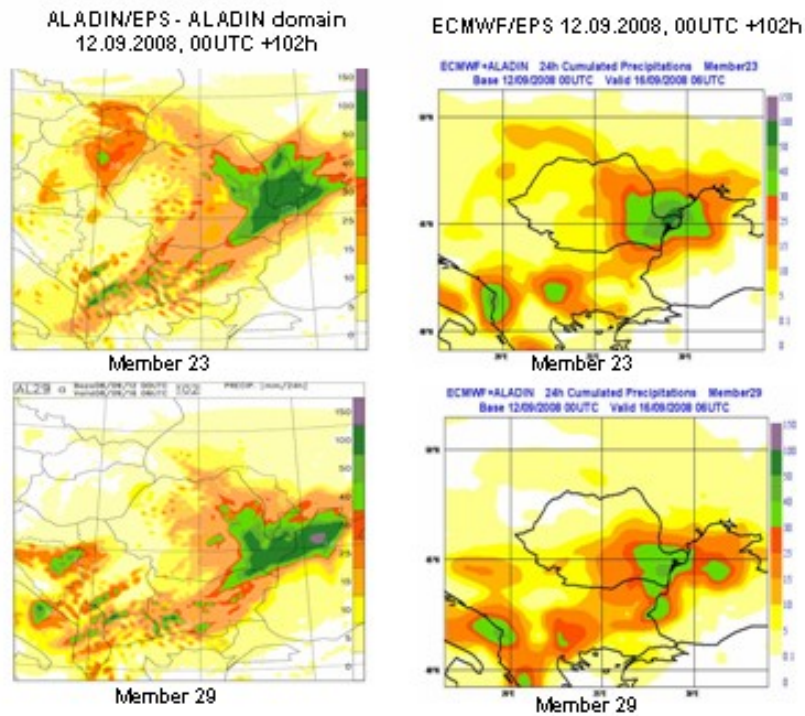


Fig.5 24 hour cumulated precipitation:15.09.2008, 06 UTC -16.09.2008, 06 UTC for the 102 hour (started at 12.109.2008, 00 UTC) ALADIN (left) and ECMF(right) forecast integrated over the ALADIN-ROMANIA domain, for the best members: 23 - first row) and 29- second row

4.1.3. Prognostic entrainment rate in ALARO (D. Banciu)

After introducing the modulation of the two antagonist terms (the downdraft dissipation term and the downdraft fractional area term) in the evolution equation of the prognostic variable, the tuning of the free parameters was done again. The results obtained for the best tuning are presented in figures 6 and 7 in comparison with the diagnostic entrainment.

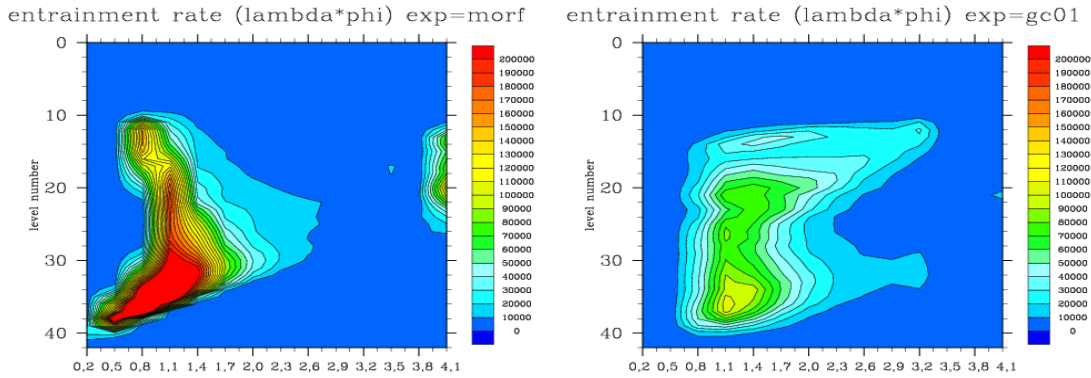


Fig.6 The vertical distribution of the scaled entrainment rate of ALARO model (including 3MT) for a period of 6 hours (between 6 and 12 forecast range to eliminate the spin up); diagnostic entrainment - left, prognostic entrainment right

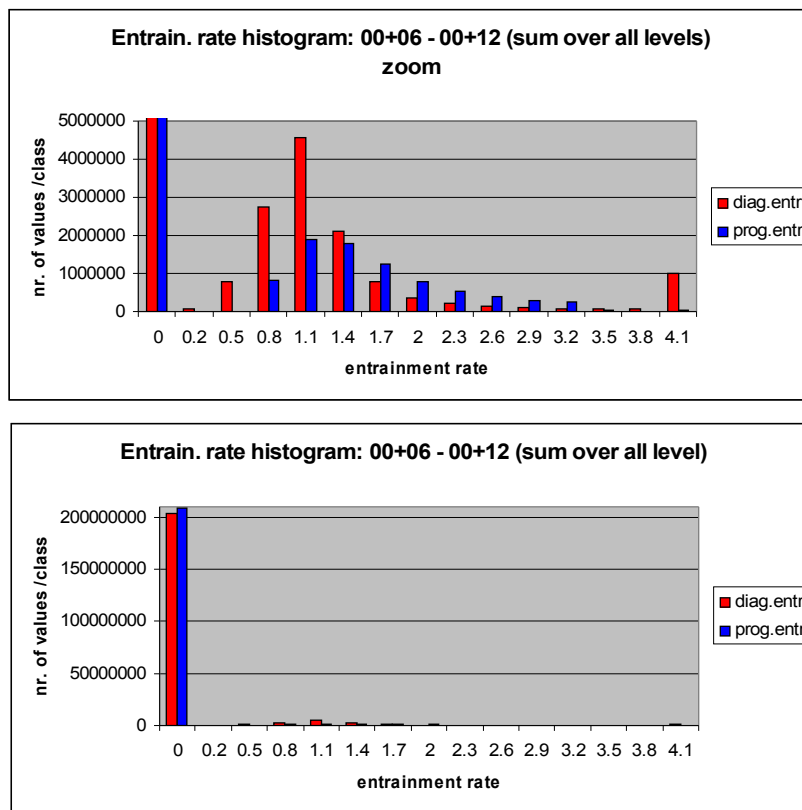


Fig.7 ALARO model (including 3MT): the scaled entrainment rate histograms over all levels for the same period of 6 hours as in figure 6: diagnostic entrainment - red, prognostic entrainment blue. Top – the entire domain of variation, bottom – a zoom.

They show that, for the prognostic entrainment in comparison with the diagnostic one, there is:

- ◆ not enough convection: the number of values in class "0" is 209118446 with respect to the diagnostic configuration, 204004341:

- ◆ a different distribution (per levels and on the level sum) of the entrainment rate over the considered interval of the entrainment rate (0-4.1).

Following this, some improvement was sought by initializing the value of the historic entrainment by the corresponding diagnostic value and its re-initialization every time when there was not physical solution. In this way, an additional reduction of the number of points without convection (up to 207391653) was obtained while the good distribution of the entrainment rate on the vertical was preserved (see figure 8).

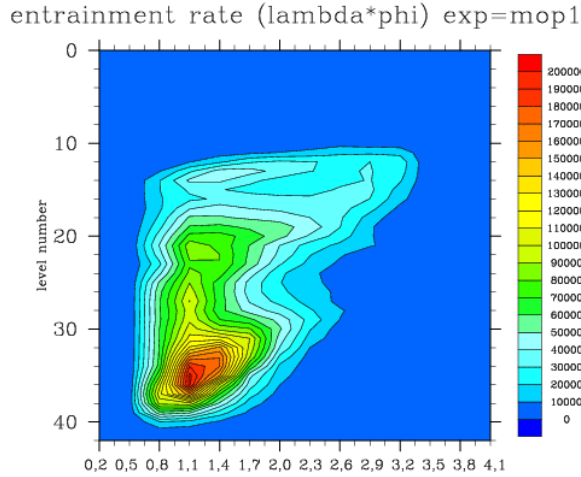


Fig.8 ALARO model (including 3MT): the vertical distribution of the scaled entrainment rate for a period of 6 hours (21.06.2006 00+06 -> 00+12 h UTC) using the prognostic entrainment with the re-initialization procedure.

New entrainment rate diagnostics have been carried out and compared with the vertical structure of the mass flux, which, in the case of the prognostic entrainment, are not correlated through the evolution equations.

The structure of the gradient of the mass flux (the part corresponding to the entrainment) and of the entrainment rate flux are globally (average over the domain for the first 12 hours of integration) similar as one can notice in figures 9 and 10, proving the realism of the prognostic entrainment formulation.

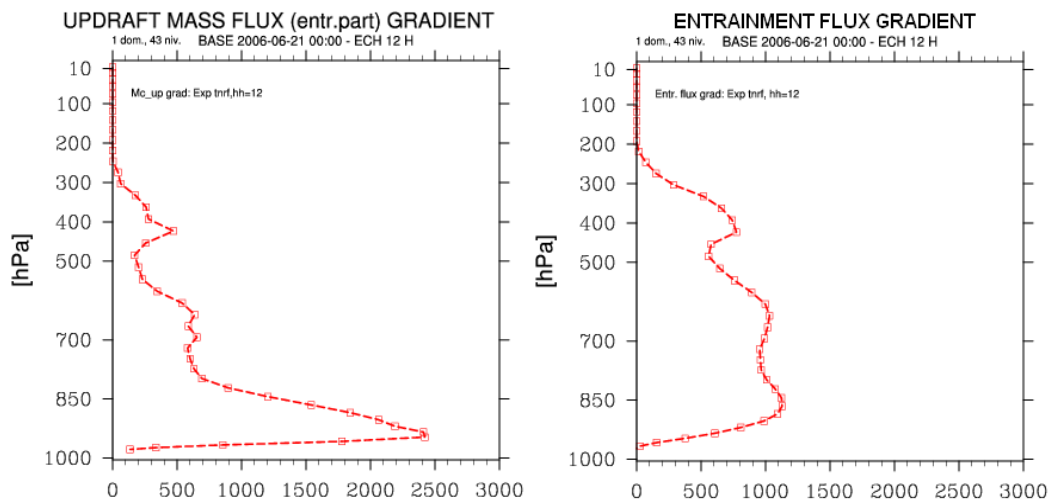


Fig.9 ALARO (including 3MT) – diagnostic entrainment: gradient of the mass flux (the part corresponding to entrainment) – left and of the entrainment rate flux – right, 6 hour cumulation (21.06.2006 00+06 -> 00+12 h UTC)

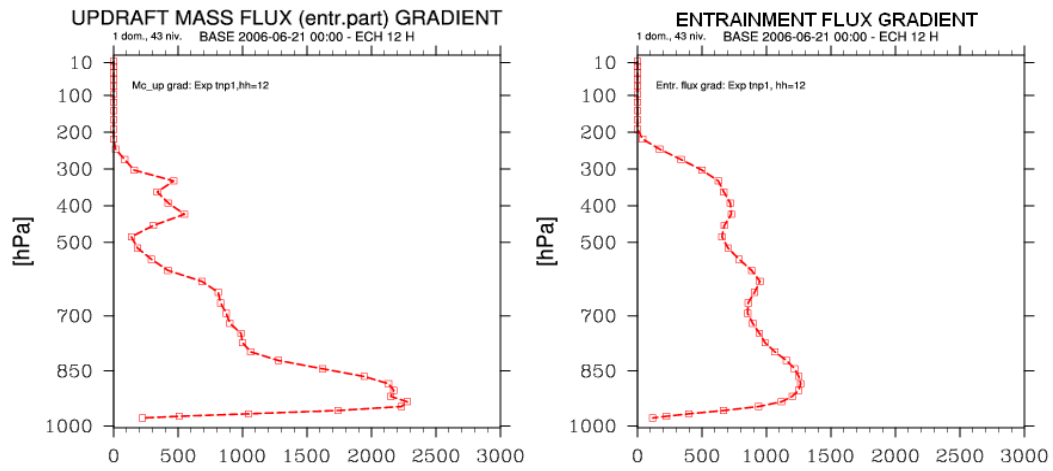


Fig.10 ALARO (including 3MT) – prognostic entrainment: gradient of the mass flux (the part corresponding to entrainment) – left and of the entrainment rate flux – right, 6 hour cumulation (21.06.2006 00+06 -> 00+12 h UTC)

4.2. SLOVAKIA

The Slovaks are very operational indeed.





5. PAPERS and ARTICLES

5.1. The application of the Ensemble Transform Kalman Filter technique in the ALADIN 3D-VAR system in Hungary*

Edit Adamcsek**, Gergely Bölöni, Petra Csomós, András Horányi

5.1.1. Introduction

The Hungarian Meteorological Service (HMS) uses operationally the ALADIN 3D-VAR data assimilation system. For the time being, background errors are considered to be constant in time and they are computed from a relatively small ensemble of ALADIN forecasts valid over an early spring period (Bölöni, 2006). However, background forecasts might be of a fluctuating quality depending on the season and on the weather situation. The Kalman Filter approach takes into account the time dependency of the background errors in the analysis cycle by the evolution of the background error covariance matrix from one analysis time step to another. The implementation of the Kalman Filter, however, is extremely expensive for large dimensional systems such as numerical weather prediction models, which excludes the possibility of a real time operational application with the currently available computer technology. In order to reduce the computing costs, ensemble methods have been introduced, where the background error covariance matrix is estimated from a small size sample of background forecasts. Different approaches exist for the generation of the perturbations for the ensembles. At the Hungarian Meteorological Service, the so-called Ensemble Transform Kalman Filter (ETKF) method has been chosen for implementation. The aim of this article is to outline the theoretical background of this technique and present the initial experiments.

5.1.2. The Kalman Filter

Data assimilation systems provide the initial conditions for NWP models by using the actual observations and a background forecast valid at the analysis time as primary information for the assimilation procedure. Optimal least-square and variational data assimilation methods estimate the true state of the atmosphere given by the analysis using the so-called BLUE (Best Linear Unbiased Estimation) estimation (Bouttier and Courtier, 1999):

$$\mathbf{x}_a = \mathbf{x}_f + P_f H^T (H P_f H^T + P_o)^{-1} (\mathbf{y} - \mathcal{H}(\mathbf{x}_f)). \quad (1)$$

Here \mathbf{x}_a and \mathbf{x}_f denote the analysis and background fields respectively, \mathbf{y} denotes the observations. Let n be the degree of freedom of the NWP model ($n \approx 10^7$, typically the number of variables to be determined for the entire model grid) and let p be the number of observations ($p \approx 10^4 - 10^6$). Then \mathbf{x}_f and \mathbf{x}_a are vectors of size n , and \mathbf{y} is a vector of size p . \mathcal{H} denotes the observation operator, which maps the state variables on the model grid to the observational points, and H is its linearized counterpart around the background state \mathbf{x}_f ($H = \frac{\partial \mathcal{H}}{\partial \mathbf{x}}(\mathbf{x}_f)$). Let $K = P_f H^T (H P_f H^T + P_o)^{-1}$, which is called the gain or weight matrix.

The P_f and P_o , background and observation error covariance matrices are defined as follows:

$$P_f := E(\boldsymbol{\varepsilon}_f \boldsymbol{\varepsilon}_f^T) \text{ and } P_o := E(\boldsymbol{\varepsilon}_o \boldsymbol{\varepsilon}_o^T), \quad (2)$$

* This article is a shortened version of a manuscript sent to Időjárás, the quarterly journal of HMS

** Corresponding author: Edit Adamcsek, Hungarian Meteorological Service, Division for Numerical Modelling and Climate Dynamics, email: adamcsek.e@met.hu

where $E(\cdot)$ denotes the expected value, $\varepsilon_f = x_t - x_f$ and $\varepsilon_o = \mathcal{H}(x_t) - y$ stand for the background and observation errors respectively where x_t is the unknown, true state of the atmosphere. Further assumptions on the errors are:

- a) The expected value of each error is zero, i.e. $E(\varepsilon_f) = E(\varepsilon_o) = 0$ (the corresponding estimate is unbiased, i.e. it does not contain any systematic error).
- b) The errors in the background state and the observational errors are uncorrelated, i.e. $E(\varepsilon_f \varepsilon_o) = 0$.

Similarly to (2), the analysis error covariance matrix can be defined as

$$P_a := E(\varepsilon_a \varepsilon_a^T), \quad (3)$$

where $\varepsilon_a = x_t - x_a$. In an assimilation system based on (1), the following relation is valid between the analysis and the background error covariance matrices (*Bouttier and Courtier, 1999*):

$$P_a = (I - KH)P_f, \quad (4)$$

where I denotes the identity matrix.

In practice, the P_f background error covariance matrix is often assumed to be constant in time in data assimilation systems, however, it is rather well known that background errors depend on the actual weather situation to a great extent, therefore it is desirable to release this consideration. The main idea of the Kalman Filter methods is to update matrix P_f at each analysis step. The standard Kalman Filter method was introduced by *Rudolf Emil Kalman (1960)*, he has shown that the following equation can be derived for the forecast error covariance matrix at time t_i :

$$P_f(t_i) = M_{i-1}^i P_a(t_{i-1}) M_{i-1}^{i-1} + P_M(t_i), \quad (5)$$

where M_{i-1}^i is the linear model forecast operator from time $i-1$ to i (i.e. a matrix of size $n \times n$), $P_a(t_{i-1})$ is the analysis error covariance matrix at time t_{i-1} and $P_M(t_i)$ is the covariance matrix of the linear model error at t_i . Updating the P_f matrix based on equation (5) is computationally expensive. The evolution of the error covariance matrix requires at least $2n$ model integrations and the storage of matrices of dimension $n \times n$, which is not practically tractable for an operational model, where $n \approx 10^7$. In order to overcome these difficulties ensemble techniques were introduced.

5.1.3. Ensemble Transform Kalman Filter

The Ensemble Transform Kalman Filter is an approximation to the traditional Kalman Filter. It uses an ensemble (i.e. a statistical population) to estimate the error covariance matrices P_a and P_f . The matrix P_a can be estimated for k ensemble members as follows (see *Houtekamer and Mitchell (2001)*):

$$P_a \approx \frac{1}{k-1} \sum_{j=1}^k (x_{a,j} - \bar{x}_a)(x_{a,j} - \bar{x}_a)^T. \quad (6)$$

Let us consider

$$Z_a = \frac{1}{\sqrt{k-1}} (z_{a,1}, z_{a,2}, \dots, z_{a,k}), \quad (7)$$

the matrix of size $n \times k$, where the $z_{a,j} = x_{a,j} - \bar{x}_a$ ($j = 1, \dots, k$) values are the analysis dispersions, i.e. the differences between the j th member $x_{a,j}$ and the ensemble average \bar{x}_a . Note, that with this notation the analysis error covariance matrix P_a can be written from equation (6) as:

$$P_a = Z_a Z_a^T, \quad (8)$$

which is the product of matrix Z_a and its transpose. Then one can assume that the background dispersions are obtained by integrating the analysis dispersions with the linear model, that is, neglecting the time index in the notation:

$$Z_f = M Z_a \quad (9)$$

and then

$$P_f = Z_f Z_f^T = M Z_a Z_a^T M^T = M P_a M^T, \quad (10)$$

hence, we get back the formula (5) of the Kalman Filter (neglecting the model error's covariance matrix P_M). In the case of ETKF instead of making k integrations, a relationship is assumed between the dispersions of the analysis and the dispersions of the background, that is

$$Z_a = Z_f T, \quad (11)$$

where $Z_f = \frac{1}{\sqrt{k-1}} (z_{f,1}, z_{f,2}, \dots, z_{f,k})$ contains the background dispersions $z_{f,j} = x_{f,j} - \bar{x}_f$ ($j = 1, \dots, k$), and T denotes the (for the time being unknown) transformation matrix of size $k \times k$ describing this relationship.

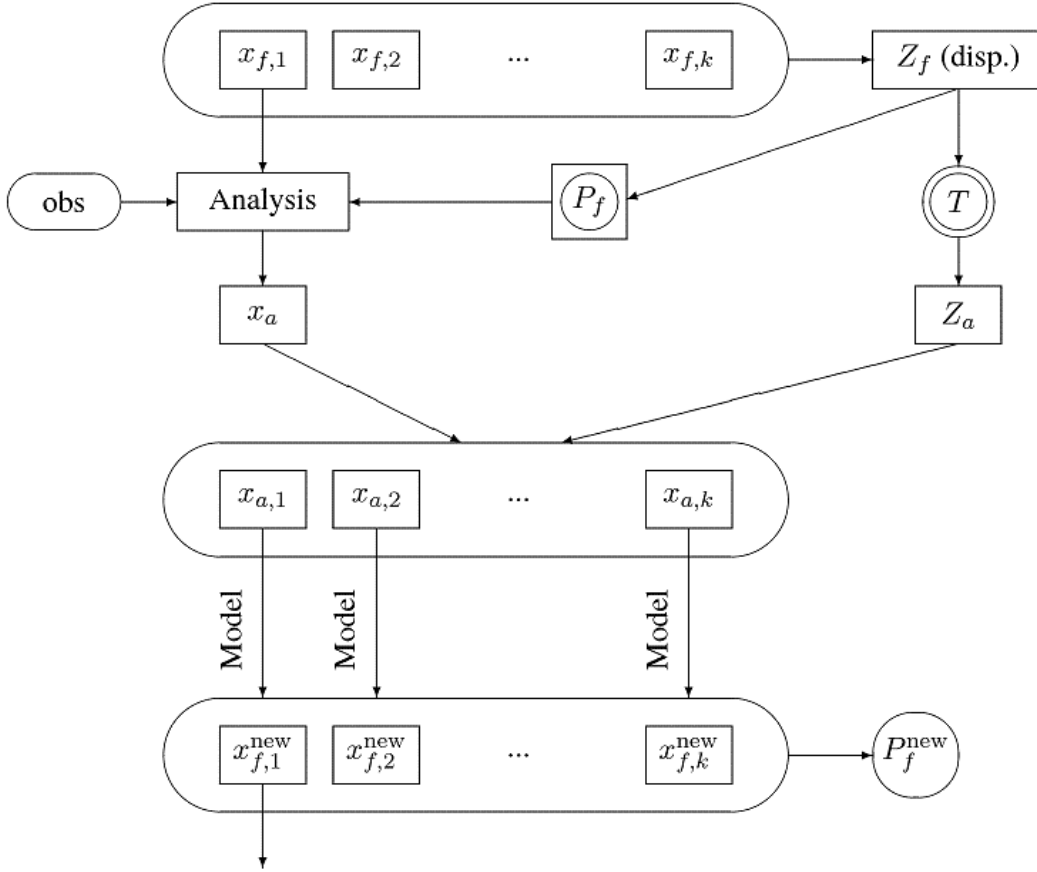


Figure 1. The schematic algorithm of the Ensemble Transform Kalman Filter.

The Ensemble Transform Kalman Filter method (the schematic algorithm can be seen on *Figure 1*.) provides an ensemble generation scheme so as to estimate the background error covariance matrix by the covariance matrix of the ensemble forecast perturbations. Let us assume that k ($x_{f,1}, \dots, x_{f,k}$) forecasts have been created at the initial time. Then the matrix of the dispersions Z_f can be computed. The algorithm transforms forecast perturbations into analysis perturbations by the transformation matrix, whose derivation is shown in the next Section. The matrix $Z_a = Z_f T$ contains the dispersions to be added to the analysis x_a computed from the control member (e.g. $x_{f,1}$). The new background members $x_{f,j}^{new}$ are determined by integrating the model with the new analysis ensemble members $x_{a,j}$ ($j = 1, \dots, k$) as initial states. From their dispersions the new values of the P_f matrix can be computed, then the procedure can restart.

5.1.4. The transformation matrix

According to the Ensemble Transform Kalman Filter method the transformation matrix T is derived from the error covariance update equation (4) provided that the matrix of background dispersions is the square-root of the background error covariance matrix. Hence, matrix T can be determined based on the following formulas (equations (11), (4) and (10)):

- $Z_a = Z_f T$,
- $P_a = (I - KH)P_f$, where $K = P_f H^T (H P_f H^T + P_o)^{-1}$,

- $P_f = Z_f Z_f^T$.

Bishop et al. (2001) showed that according to the above assumptions matrix T can be determined as:

$$T = C(\Gamma + I)^{-1/2}, \quad (12)$$

where

$$Z_f^T H^T P_o^{-1} H Z_f = C \Gamma C^T. \quad (13)$$

Thus, matrix C contains the normalized eigenvectors of matrix $Z_f^T H^T P_o^{-1} H Z_f$, and the diagonal Γ matrix contains the corresponding eigenvalues.

The analysis perturbations $z_{a,j}$ obtained by the use of this T matrix are not centered around their mean, so the mean of the generated ensemble won't be identical to the analysis x_a . Ideally, one would like the ensemble mean to be equal to the best available estimate of the true state, that is, the analysis. Therefore a centering method is required, which is to post-multiply the transformation matrix T by C^T to form the new, centered analysis dispersions: $Z_a = Z_f T C^T$ (*Wang et al.*, 2004). Hence, matrix T can be obtained as

$$T = C(\Gamma + I)^{-1/2} C^T. \quad (14)$$

However when the size of the ensemble k is significantly smaller than the rank of the true forecast-error covariance, $P_a = Z_a Z_a^T$ underestimates total analysis error variance. To increase the ensemble covariance the inflation method is used, the analysis perturbations are multiplied by an estimated inflation factor, Π :

$$Z_a = Z_f T \Pi. \quad (15)$$

The derivation of the estimation of the inflation factor can be read in the next Section. Now the transformation matrix is computed:

$$T = C(\Gamma + I)^{-1/2} C^T \Pi. \quad (16)$$

5.1.5. Estimation of the inflation factor

The objective of the inflation method is to insure that the background ensemble variance (P_f) is consistent with the control forecast error. In order to insure this consistency *Wang and Bishop* (2003) proposed to apply the following equation derived by *Desroziers et al.* (2005):

$$E(dd^T) = P_o + H P_f H^T, \quad (17)$$

where $d = y - H(x_f)$ is the innovation vector: the difference of the observation vector y and its background counterpart $H(x_f)$, that is the background forecast mapped into the observation space. Now define \tilde{d}_i as the innovation vector at t_i , normalized by the square root of the observation

error covariance matrix, that is, $\tilde{d}_i = P_o^{-1/2}(y_i - H(x_i^f))$, where the index i denotes the time t_i . Let \tilde{H} be the observation operator normalized by the square root of the observation error covariance matrix, $\tilde{H} = P_o^{-1/2}H$. Now Eq.(17) can be written as:

$$E(\tilde{d}_i \tilde{d}_i^T) = I + \tilde{H}P_f(t_i)\tilde{H}^T, \quad (18)$$

where $P_f(t_i)$ indicates the background error covariance matrix estimated from the forecast ensemble at t_i . For the estimation of the inflation factor this formula can be simplified as *Wang and Bishop* (2003) proposed:

$$\tilde{d}_i^T \tilde{d}_i = \text{trace}(I + \tilde{H}P_f(t_i)\tilde{H}^T). \quad (19)$$

Though the inflation computed at time t_i needs to insure the consistency for the next forecast, which is valid at t_{i+1} , the data of that ($\tilde{d}_{i+1}^T \tilde{d}_{i+1}$ and $\text{trace}(I + \tilde{H}P_f(t_{i+1})\tilde{H}^T)$) is not available at the update time t_i . Therefore one assumes that the error statistics of the next forecast will be similar to that of the one at t_i , which may be a good approximation since the time interval between t_i and t_{i+1} is 6 hours in our experiments. Now the inflation factor is obtained by checking if $\tilde{d}_i^T \tilde{d}_i$ is equal to $\text{trace}(I + \tilde{H}P_f(t_i)\tilde{H}^T)$. If not, an inflation factor is needed: $Z_a = Z_f T \Pi_i$. Since $Z_f T \Pi_i = Z_f \Pi_i T$, the inflated ensemble covariance matrix is $(Z_f \Pi_i)^T Z_f \Pi_i = \Pi_i^T Z_f^T Z_f = \Pi_i^2 P_f(t_i)$. To make equation (19) hold, the inflated covariance matrix is to be used, and the suitable inflation factor can be determined by the equation:

$$\tilde{d}_i^T \tilde{d}_i = \text{trace}(I + \tilde{H}\Pi_i^2 P_f(t_i)\tilde{H}^T). \quad (20)$$

From (20) using (13) we obtain:

$$\Pi_i = \sqrt{\frac{\tilde{d}_i^T \tilde{d}_i - p}{\sum_{j=1}^{k-1} \lambda_j}}, \quad (21)$$

where p is the number of observations and $\lambda_j, j = 1, \dots, k - 1$, are the diagonal elements of Γ .

5.1.6. Preliminary experiments

The preliminary experiments with ETKF were embedded into the operational environment. The ETKF system needs an initial forecast ensemble, which was provided by the operational LAMEPS (Limited Area Model Ensemble Prediction System) used at HMS, which is the downscaling of the singular vector (SV) based global ensemble system PEARP (Prévision d'Ensemble ARPege) (*Hågel and Mile*, 2009). The members of the same LAMEPS system were used as lateral boundary conditions (LBCs) for ETKF. As this particular ensemble includes one control forecast $x_{f,1}$ and ten perturbed members ($x_{f,2}, \dots, x_{f,11}$), the ensemble size was chosen as 11 in the experiments as well.

Although the ultimate goal is to make the background error covariance matrix P_f flow-dependent, in these first experiments as it was not yet updated with the help of the ETKF ensemble,

it was the same as the one used in operations in all analysis time. The test was run from 00 UTC 3 September to 18 UTC 9 September 2008, which is a randomly chosen period, with a 6 hour cycling frequency in agreement with the operational data assimilation cycling setup at HMS. As already mentioned above, the LBCs were taken from the operational LAMEPS system. Thus a sufficient sample of the analysis and the background dispersions was collected for their statistical analysis.

In order to study the influence of the inflation factor on the perturbations, the following two experiments were run. In the first one – taken as reference - there was no inflation used. In the second one the inflation factor was estimated in each analysis time as described above (the initial inflation factor was chosen as 10) and built into the transformation matrix. In these tests the main intention was to focus purely on the impact of the inflation on the perturbations, therefore the LBCs were kept constant for all the ETKF members, i.e. all of them were coupled to the same LAMEPS control member. For the evaluation of forecast dispersions the rank histograms (also known as Talagrand diagrams) were examined. These histograms were generated by verifying the forecast ensembles against ECMWF (European Centre for Medium-Range Weather Forecasts) analysis. In *Figure 2* the Talagrand diagram for the background ensembles are shown without and with inflation. It is obvious that the extreme ranks are overpopulated, which indicates that there is a lack of variability in the ensemble, i.e. the background ensemble statistically underestimates or overestimates the truth. As some values appear in the middle ranks on the right panel in *Figure 2*, the inflation had some minor impact on the variability, but it did not change the spread significantly. In order to gain additional variability in the background ensemble, it was decided that the LBCs should also be perturbed.

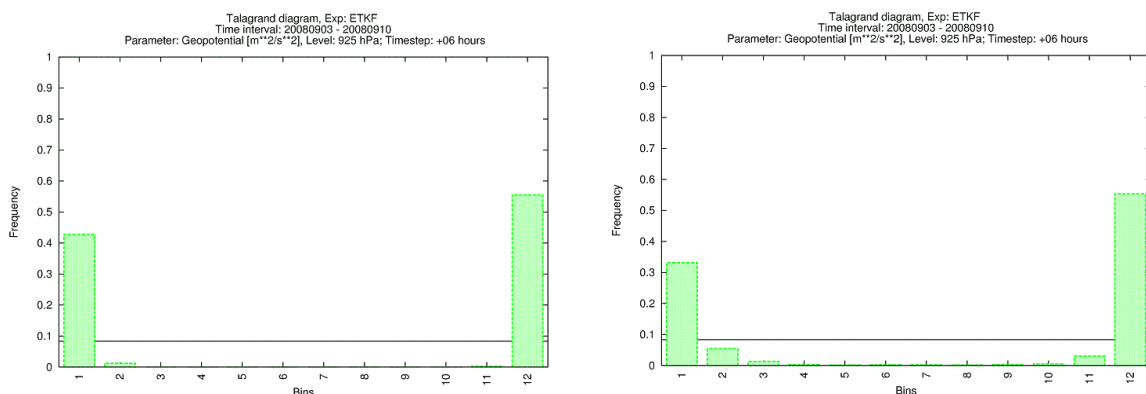


Figure 2. Talagrand diagrams for forecast ensembles generated without inflation (left) and with inflation (right) for the period 00UTC 3 September to 18 UTC 9 September 2008 for 925hPa geopotential

In a limited area model, such as ALADIN, forecasts depend a lot not only on the initial, but also on the lateral boundary conditions. Thus, in this experiment, uncertainties through LBCs were also included besides the initial perturbations. This was achieved by coupling each member of the background forecast ensemble with a different member of the PEARP global system. It must be said that there is an inconsistency in this approach, since the perturbation generation methods are fundamentally different in a global and in a LAM system, the PEARP system applies the SV method and not ETKF. This coupling strategy was a technical constraint given the fact that no access to any global ETKF ensemble system was available. On the other hand the effect of this inconsistency on our experiments is unknown. Both the inflated and the non inflated ETKF cycles were rerun with perturbed LBCs. The corresponding Talagrand diagrams are shown in Figure 3. In both inflated and non inflated cases, the middle ranks are much more populated compared to the previous test. This indicates that the perturbation of the LBCs increases more widely the ensemble spread than the applied inflation method itself. However, it is to be noticed that the Talagrand diagram still shows a U profile, which means that the ensemble does not reflect the true state in spite of the perturbed LBC. This finding suggests that the LBCs are not the only factors in the forecast uncertainties and

most probably there is still room for improvement in the construction of the initial conditions in order to have a better spread of the forecast ensemble. Therefore it can be concluded that further development of the ETKF transformation needs to be made in order to improve the initial conditions.

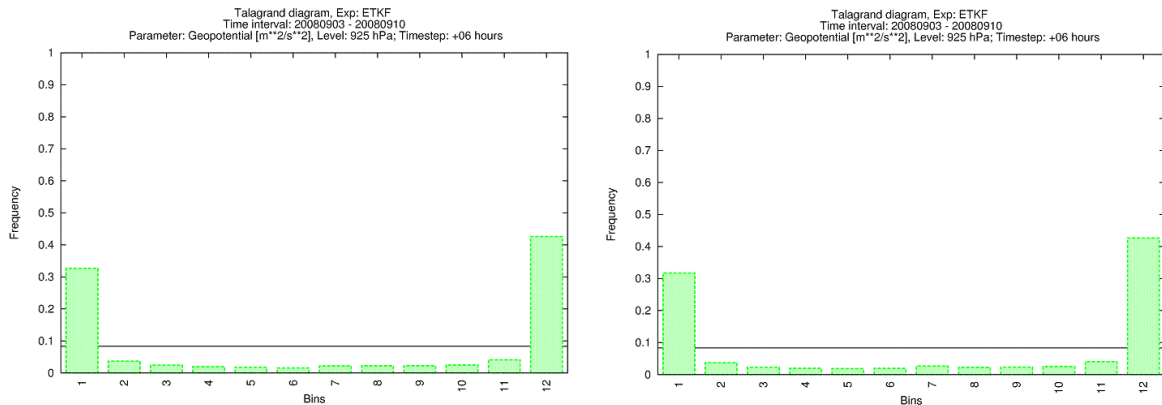


Figure 3. Talagrand diagrams for forecast ensembles created with perturbed LBCs for the period 00UTC 3 September to 18 UTC 9 September 2008 for 925hPa geopotential. The ensembles were generated without inflation (left) and with inflation (right).

5.1.7. Summary and discussion

The primary objective of the application of the Ensemble Transform Kalman Filter (ETKF) method at the Hungarian Meteorological Service is to compute flow-dependent background errors for the operational ALADIN 3D-VAR data assimilation system. Hence the implementation was embedded into the operational version of the ALADIN model in Hungary. Yet, this paper concentrates on the preliminary testing of the ETKF algorithm and performs the first, basic validations of the system.

Tests were carried out to understand the impact of inflation in an ETKF cycling environment (but keeping the background errors constant in time). A 7 days period was randomly chosen and the ensemble spread of the background errors was diagnosed with the help of Talagrand diagrams. The Talagrand diagram diagnostics clearly indicated that the spread of the analysis and forecast ensembles were insufficient in spite of the fact that the inflation slightly improved the characteristics of the forecast ensemble. It has been shown that the perturbed lateral boundary conditions further improved the spread of the ensemble, however it was still far from being optimal. This latter finding indicates that there is still room for improvements in the initial analyses of perturbations with the application of a more optimal inflation factor.

While investigating the results one has to think of the proper diagnostics to be used to evaluate the quality of the ETKF ensemble. It has to be kept in mind that the primary goal for the ensemble generation is to provide a sample of forecast differences for the computation of a time-dependent P_f matrix at every assimilation step. This implies that a background ensemble is required with a variable spread depending on the quality and reliability of the actual background forecast. In other words, when the background forecast is good (bad) the ETKF ensemble must have a small (large) spread implying small (large) error variances and covariances in P_f . Unfortunately the Talagrand diagram diagnostics do not reflect exactly this information but rather show whether or not the ensemble represents the observed weather. In the future, for better diagnostics it is intended to compute the spread-skill relationship, which normally compares the root mean square error (RMSE) of the ensemble mean with the ensemble spread. Instead of the RMSE of the ensemble mean it is planned to use the RMSE of the control member, which is used in the 3D-VAR analysis. It is believed that this might give a better insight into the characteristics of the ensemble forecasts used

in the ETKF procedure.

Otherwise the insufficient spread in the ETKF ensemble might have several sources. One of the reasons may be the operational environment that was used in the implementation. The ETKF study made by *Wang and Bishop (2003)* showed good results in a simplified experimental setup assuming that the number, quality and location of observations are similar at all analysis times, while none of these assumptions are met in an operational data assimilation system. The inflation method was derived by assuming that the error statistics are not changing from one analysis time to the other, so this inflation strategy needs to be modified in an operational system.

Another potential cause of the small spread of the ETKF implementation is that in the experiments the P_f matrix was not updated using the generated forecast ensemble, although it is assumed in the ETKF theory. This inconsistent setup was due to the fact that an ensemble size of eleven does not provide a sufficient sample to compute a P_f matrix. One possibility would be to increase the ensemble size, however this could not be feasible in an operational framework with the present available computational resources. Two other options would be to accumulate the ensemble dispersions over several analysis times or to construct a so-called hybrid P_f matrix with a climatological and a flow-dependent component where the first would come from a long time accumulation and the latter from the actual analysis time. Both of these solutions would however weaken the flow-dependence of P_f . Therefore a future challenge will be to find an affordable solution that keeps the dependence of the background errors on the actual weather.

References

- C. H. Bishop, B. J. Etherton, and S. J. Majumdar, 2001: Adaptive sampling with the Ensemble Kalman Transform Filter. Part I: Theoretical aspects. *Monthly Weather Review* 129, 420-436.
- F. Bouttier and Ph. Courtier, 1999: Data assimilation concepts and methods. ECMWF Meteorological Training Course Lecture Series
http://www.ecmwf.int/newsevents/training/rcourse_notes/DATA_ASSIMILATION/ASSIM_CONCEPTS/Assim_concepts.html
- G. Bölöni, 2006: Development of a variational data assimilation system for a limited area model at the Hungarian Meteorological Service. *Időjárás* 110, 309-328.
- G. Desroziers, L. Berre, B. Chapnik and P. Poli, 2005: Diagnosis of observation, background and analysis error statistics in observation space. *Quarterly Journal of the Royal Meteorological Society* 131, 3385-3396.
- E. Hágel and M. Mile, 2009: The limited area ensemble prediction system of the Hungarian Meteorological Service. *ALADIN Newsletter* 35.
- P. L. Houtekamer and H. L. Mitchell, 2001: A sequential ensemble Kalman filter for atmospheric data assimilation. *Monthly Weather Review* 129, 123-137.
- R. E. Kalman, 1960: A new approach to linear filtering and prediction problems. *ASME Journal of Basic Engineering* 82, 35-45.
- X. Wang, C. H. Bishop, S. J. Julier, 2004: Which Is Better, an Ensemble of Positive-Negative Pairs or a Centered Spherical Simplex Ensemble? *Monthly Weather Review* 132, 1590-1605.
- X. Wang, C. H. Bishop, 2003: A Comparison of Breeding and Ensemble Transform Kalman Filter Ensemble Forecast Schemes. *Journal of the Atmospheric Sciences* 60, 1140-1158.

5.2. Forecasting Tropical Cyclones using ALADIN

Ghislain Faure and Matthieu Plu

Météo-France, Laboratoire de l'Atmosphère et des Cyclones (LACy)

UMR 8105 CNRS / Météo-France / Université de La Réunion

5.2.1. Aladin-Réunion outlook

The numerical prediction of tropical cyclones is a concern for Météo-France, mainly because of its WMO responsibilities. Indeed, Météo-France at La Réunion is the Regional Specialized Meteorological Centre (RSMC) for tropical cyclones over the South-West Indian Ocean (SWIO). At La Réunion, Météo-France and LACy (the joint lab between CNRS, Météo-France and the local University) host a research unit on tropical cyclones. One of its mission is to develop some methods and models dedicated to operational forecasting of tropical cyclones. An operational Aladin 3D-Var has been considered as a very promising model since 2004 (Willemet et al, 2004). After several years of development, such a model was put into operations on the Météo-France supercomputer in Toulouse, under the name Aladin-Réunion (Faure et al., 2008).

Initially adapted from Aladin-France, the model has inherited from it its main characteristics, including the 3D Var assimilation scheme and the Lopez microphysics. Aladin-Réunion is also coupled to Arpege.

However, running Aladin over a tropical domain induces two specificities that are also two major concerns for tropical cyclone initialization and modelling. The first one is the lack of in-situ observations, with a limited-area domain (Fig.1) mostly over ocean. In addition, the available observation networks over emerged land are far from being dense, excepted on La Réunion tiny island. The second specificity is the importance of air-sea interactions, 90% of the surface gridpoints being over sea.

In addition to the lack of in-situ observations, virtually no satellite observations in the vicinity of a cyclone are assimilated by the current Aladin-Réunion 3D-Var (Fig. 2), due to cloud and rain contamination. An alternative to obtaining good tropical cyclone forecast skills where very few observations are available for assimilation, is to provide a realistic 3D wind vortex to the minimisation, through pseudo-observations or “bogus” (Montroty et al., 2008, for more details). Creating these observations relies primarily on a tropical cyclone analysis by a forecaster, which provides localization and intensity thanks to the Dvorak technique. Then a 2D analytic model of wind distribution (Holland, 1980) is applied, and then it is extrapolated on several vertical levels. The final 3D vortex (crosses in Fig.2) is defined horizontally with two circles, of 100km and 200km radii, gathering 8 observations each. Vertically, it goes from 10m up to 500 hPa through 4 layers.

As for air-sea exchanges, Aladin-Réunion like Aladin-France, uses the ECUME parametrisation for surface turbulent fluxes, but the neutral exchange coefficient formulation differs for the latent heat. The use of the Aladin France coefficient, which produce higher flux values, generates too intense cyclones, sometimes by as much as 40hPa!

5.2.2. Operational performance during the cyclone season 2008-2009

Aladin-Réunion has been operational for 3 cyclone seasons. Since 2006, the model has greatly improved: its vertical resolution has been refined from 41 to 60 layers, its area has been extended and the forecast lead time now goes as far as 84h. Central pressure bogus has been replaced by a more satisfactory 3D wind bogus and physical parametrisations have been enhanced (Bouteloup et al, 2008, for the latest changes). A focus on the last cyclone season will give an overview of the current operational performance of Aladin-Réunion.

The skill of tropical cyclone numerical forecasts is assessed basically by two criteria: the Direct Position Error (DPE) of the cyclone centre and the intensity error, that is measured by a

proxy such as the central pressure or the maximum wind. The capacity to forecast changes in trajectory and in intensity of a cyclone is critical for an efficient alert system *in fine*.

Fig.3a shows the mean DPE of 4 models, computed for the 5 most intense cyclones of the 2008-2009 season. Additional dispersion diagnostics are plotted ($[\text{rms DPE}]/[\text{mean DPE}]$, in %), that measures the reliability of position forecasts: a high dispersion means the predominance of large errors around the mean DPE. The most striking feature of Fig. 3a is the overall performance of the IFS model, beating the 3 other models from 18 to 72h. Aladin-Réunion and Met Office global model (using bogus too) share similar characteristics: a very low initial DPE followed by a rapid growth of error. The dispersion of error is also the lowest for the bogussed models, up to 30h lead time. Arpege, even with overall decent tracking performances, is the last of the four models for tracking cyclones during this season, both in error and dispersion (existence of several huge errors).

Fig. 3b focusses on absolute intensity errors and gives another hierarchy between these models. Aladin-Réunion has the most accurate intensity forecasts until 48h lead time (contrary to DPE, the available sample was too small for longer lead times). The dispersion of IFS and Aladin-Réunion errors are comparable and slightly higher than the two other models. Actually the latter barely intensify any cyclones due to their coarser horizontal resolutions, and thus have pretty poor, but stable over time, intensity forecasts.

Aladin-Réunion emerges as a very useful operational model for both track and intensity forecasts, even if IFS remains the worldwide top model for cyclone track forecasts (Fiorino, 2009). Obviously, this statistical approach blurs the particular behaviours that may occur on some cyclones. From this point of view, Gael (2009) is an interesting case.

5.2.3. A zoom on the intense tropical cyclone GAEL

As one of the most intense cyclone during the 2008-2009 season, Gael reached its maximum intensity on the 7th of February, with an estimated 10' sustained wind of 185km/h and gusts of 260km/h, while moving as close as 400 km from La Réunion. It was thus a challenging case for the RSMC forecasters since it threatened the island during several days. Moreover, Gael highlighted the specific behaviours of the numerical models.

Among all available models at the RSMC, Aladin-Réunion performed the best track forecasts of Gael. The successive Aladin-Réunion track forecasts (Fig. 4a) were both accurate and stable, with a remarkable prediction of the track inflexion. IFS showed less accuracy overall and more fluctuation between runs (Fig. 4b). But the intensity forecasts by Aladin-Réunion were far from perfect. Fig. 5 (bottom) shows the 10m maximum wind speed on the 5th of February 00Z runs of Aladin-Réunion, Arpege and IFS. While the two global model underestimate the cyclone intensity, Aladin-Réunion largely over-intensifies the wind speed.

Such an excessive intensification by Aladin-Réunion occurred on several Gael runs, but it has not be seen for any other cyclone during the whole season. Such an unrealistic behaviour of Aladin may have many causes, among which is the structure of the cyclone in the analysis. Due to the use of the 3D wind bogus and a not so perfect guess, the 3D Var may elaborate an unrealistic asymmetric vortex, which produces model spin-up during the first hours. To estimate the contribution of initial conditions to the over-intensification of Gael, Aladin-Réunion has been run in dynamical adaptation, either from Arpege or IFS. The maximum wind forecasts (Fig. 5, bottom) show that, even with very different initial conditions, Aladin still over-intensifies Gael. The main reason(s) of the over-intensification has(ve) then to be found elsewhere, and it is still a work under progress.

These tests of sensitivity also illustrate the benefit of the meso-scale 3D-Var in comparison to dynamical adaptation runs (Fig. 5, top). The radius of maximum wind indicates the size of the simulated vortex, and global model values are usually far from the truth, except for the largest eyes. Aladin-Réunion simulates a realistic cyclone size that remains stable with time. Conversely, Aladin

runs from dynamical adaptations (from IFS or Arpege) lose this interesting skill as they produce a large vortex which size undergoes erratic changes with time. The main explanation is probably the high spatial resolution of the 3D-Var assimilation, that is the same as forecast resolution -10km. The 4D Var schemes of IFS and of Arpege are performed at a lower resolution than the forecast, which is already coarser than Aladin's one. Finally, a large and weak vortex is produced in these global model analysis, and performing a 10km resolution Aladin forecast from such initial conditions increases the intensity but does not change the unrealistic structure. This kind of difference between cyclone forecasts starting from a high-resolution LAM 3D-Var and from dynamical adaptation from a coarse-resolution global model is not specific to Gael and it may be observed for any kind of cyclone.

5.2.4. Next improvements of Aladin-Réunion

We have previously mentioned how important air-sea interactions are for cyclone forecasts in Aladin-Réunion. Since February 2009 the parametrisation of the surface fluxes is up-to-date with the use of ECUME, but a flaw remains: the lack of an high resolution prescribed sea surface temperature (SST) field, that would rely on infra red and microwave satellite data. Actually, the accuracy of the SST field is critical for cyclone intensity forecast, and it can have a similar impact as changing the parametrisation of surface flux (Fig. 6). Several comparisons have been performed on two cyclone seasons and they all show the great utility of high resolution satellite data, particularly the microwave ones that can measure SST even in cloudy areas. The enhancement of the operational SST field would be a first step to improve cyclone intensity forecasts, before developing a coupled model between the atmosphere and the ocean. Such developments are needed to reach the state of the art in numerical models for cyclone intensity prediction.

On a shorter time-scale, Aladin-Réunion will increase both its horizontal and vertical resolutions, going from 10km L60 to 8km L70. Keeping the same domain, the number of gridpoints will increase by 82.5%. The very first experiments have been done, and they show good performance in cyclone forecasts, both in track and intensity. More details in the cyclone structure appear. Adopting a new resolution does not solve the over-intensification of Gael, but it does not worsen it though.

5.2.5. Conclusion

Aladin-Réunion has been in operations for almost three years. It has become throughout the recent cyclone seasons an useful model for the RSMC forecasters. It stands as a good alternative to the IFS excellent forecasts concerning cyclone tracks, and brings rare and valuable information on cyclone intensity and structure. However, cyclone over-intensifications may occur, and no precise explanation about this behaviour have been found yet.

The Aladin-Réunion cyclone forecast skill is expected to make progress in the short and mid term range, thanks to several improvements in the model :

- increased vertical and horizontal resolutions
- new deep convection parametrisation (3MT)
- enhanced SST field

In parallel, working on the 3D Var scheme will help to produce better balanced and more realistic analysed vortices.

Aladin-Réunion has been initially developed for cyclone forecasts, but it also gives valuable information on everyday weather prediction, especially over La Réunion which is a small and steep island. This topic will be covered in a future article.

Acknowledgements

The authors are very grateful to all the people that make Aladin-Réunion everyday forecasts possible ... and valuable: first of all the Aladin Community, and in particular all CNRM/GMAP members with whom we work (giving “name list” would be too long); Météo-France Toulouse technical divisions (with a special thanks to the COMPAS/GCO team) ; Météo-France students who are not afraid to work on this topic during 6 months at a 9000km distance from Toulouse; and people from Météo-France La Réunion - forecasters, researchers, computer specialist - with whom we fruitfully work everyday.

REFERENCE

- Bouteloup, Y., E. Bazile, F. Bouyssel and P. Marquet, 2008. Evolution of the physical parametrisations of arpege and aladin-mf models, *Aladin Newsletter*, 35, 48—57.
- Faure, G., S. Westrelin and D. Roy, 2008. Un nouveau modèle de prévision à Météo-France : Aladin-Réunion, *La Météorologie*, 8(60), 29—35. (*French only*)
- Fiorino, M., 2009. Record-setting performance of the ECMWF IFS in medium-range tropical cyclone track prediction, *ECMWF Newsletter*, 118, 20—27.
- Holland, G. J., 1980. An analytic model of the wind and pressure profiles in hurricanes, *Mon. Wea. Rev.*, 108(2), 1212—1218.
- Montroty, R., F. Rabier, S. Westrelin, G. Faure and N. Viltard, 2008. Impact of wind bogus and cloud- and rain-affected SSM/I data on tropical cyclone analyses and forecasts, *Quart. J. Roy. Meteor. Soc.*, 134, 1673—1699.
- Willemet, J.-M., and S. Westrelin, 2004. Capability of the Aladin 3D variational mesoscale assimilation scheme to simulate a cyclone in the South-West Indian Ocean, *Aladin Newsletter*, 27, 157—164.

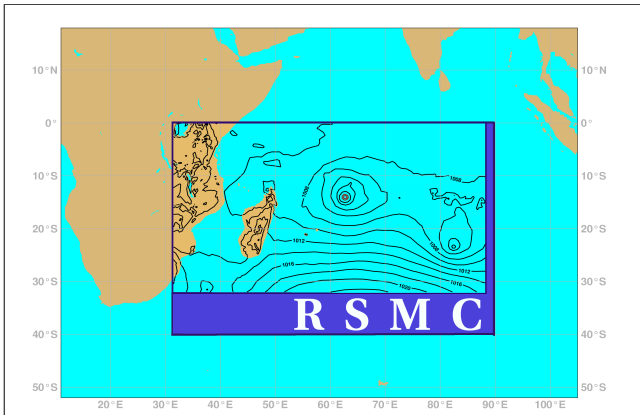


Fig.1: Responsibility area of RSMC La Réunion (deep blue rectangle), and Aladin-Réunion domain (sea level pressure field). La Réunion island is approximately 21°S and 55E.

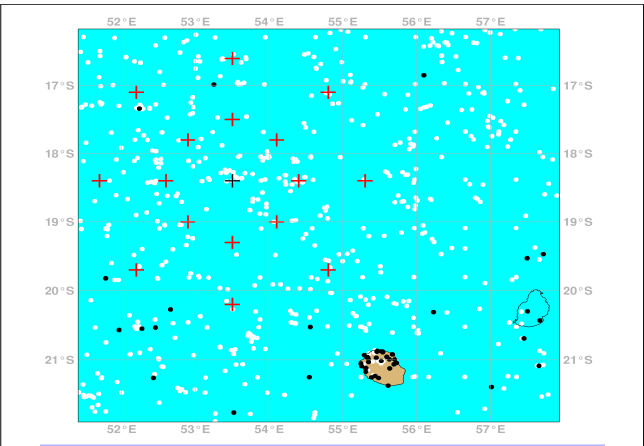


Fig. 2 : Plane projection of observations : available (white dots) and assimilated (black dots). The red crosses indicate the wind pseudo observation, the black cross being the centre of the cyclone.

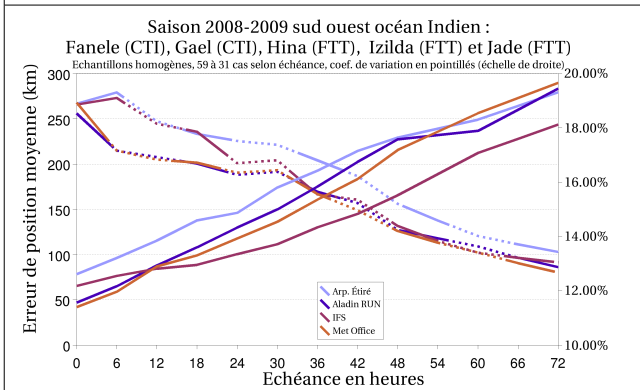


Fig. 3a : Mean Direct Position Error (plain lines, in km) and dispersion (rms DPE divided by mean DPE, in %, dot lines) for four models.

The statistics, made on 5 cyclones of the 2008-2009 season, are homogeneous between models. Sample size : between 59 and 31 according to lead time.

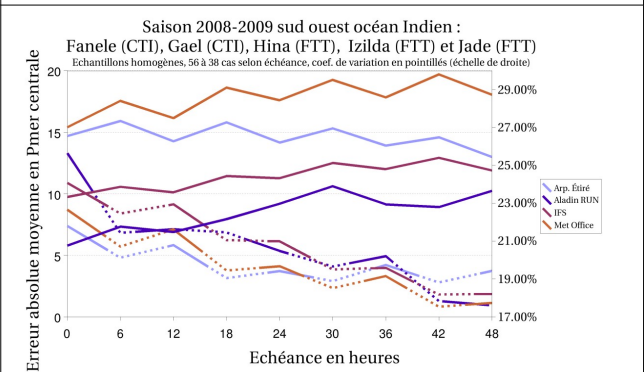


Fig. 3b : Mean absolute Central Pressure Error (plain lines, in hPa) and (rms error divided by mean error, in %, dot lines) for four models.

The statistics, made on 5 cyclones of the 2008-2009 season, are homogeneous between models. Sample size : between 56 and 38 according to lead time.

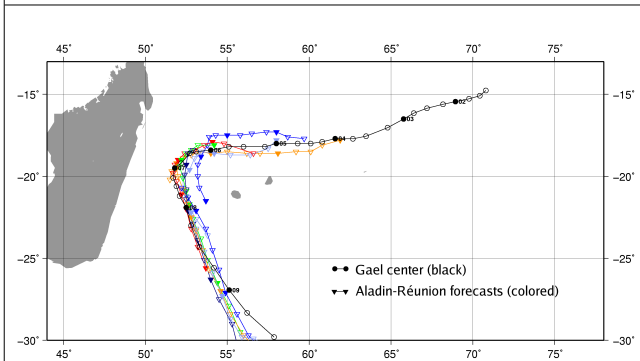


Fig. 4a : Track of Gael tropical cyclone as analysed by forecasters (black line) ; Aladin-Réunion 84h forecasts for runs between the 4th of Feb. 00Z and the 8th of Feb. 00Z (coloured lines)

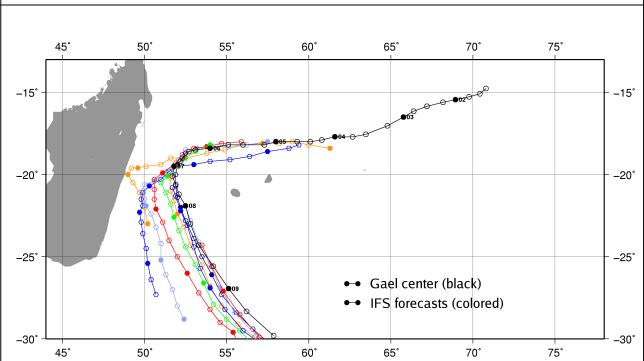


Fig. 4b : Track of Gael tropical cyclone as analysed by forecasters (black line) ; IFS 84h forecasts for runs between the 4th of Feb. 00Z and the 8th of Feb. 12Z (coloured lines)

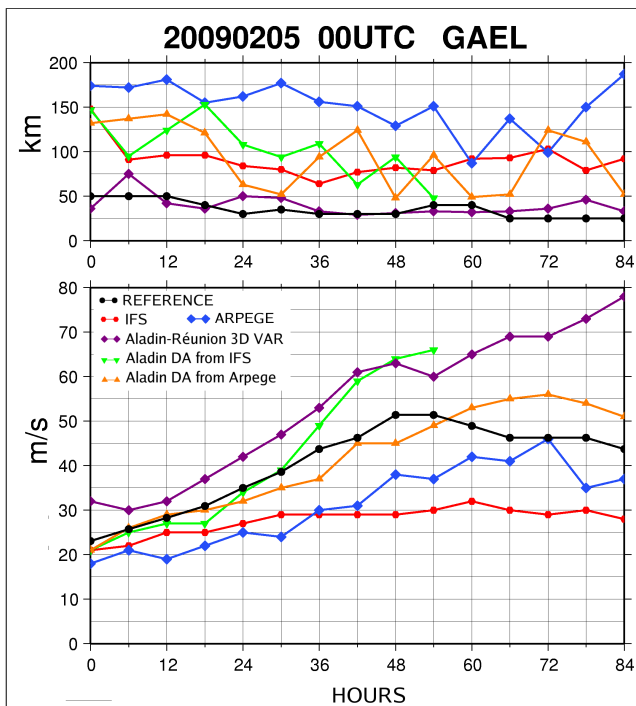


Fig. 5 : Runs on the 5th of February 00Z, by 5 models : IFS, Arpege, Aladin-Réunion 3D Var, Aladin in dynamical adaptation of Arpege, Aladin in dynamical adaptation of IFS. The reference is the black line (wind deduced from Dvorak analysis).
 Top : radius of maximum wind (in km)
 Bottom : maximum winds (in m/s)

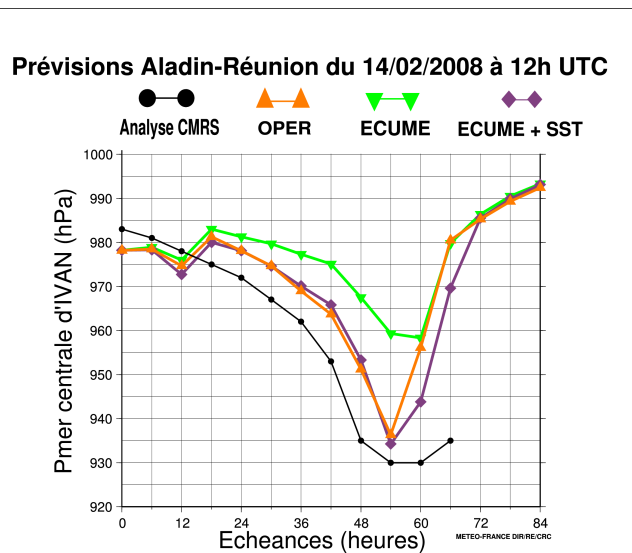


Fig. 6 : Central pressure of tropical cyclone IVAN as simulated by three Aladin-Réunion runs on the 14th of February 2008 at 12Z :
 OPER : Aladin-Réunion with Louis formulation (old one) of surface flux and basic SST field
 ECUME : same as previous but with ECUME flux parametrisation
 ECUME+SST : same as previous but with an high spatial resolution SST analysis that uses microwave satellite data (presence of a warmer area of SST on the cyclone track compared to the initial SST field)

5.3. Evaluation from large-scale to meso-scale simulated rainfall in regard to October 2008 observations.

K.ESSAOUINI

5.3.1. Introduction

The weather during the month of October 2008 was characterized by exceptionally heavy rainfall over Morocco. Over this period, the country was under tropical weather conditions characterized by hot and very humid air. The cloud systems that reached Morocco at the time were mostly convective systems. Showers from such systems were scattered, localised and hazardous all over the country especially over the mountains and surrounding areas.

The rainfall took the shape of rain or hail showers, starting and ending suddenly with big and quick variations in intensity. Usually heavy and short-lived showers were born from highly convective and unstable clouds. Thus, in some areas records were broken, with precipitations ten times the norm (over a 30 year period).

Between the 8th and the 11th of October 2008, stormy showers caused havoc and some casualties over the kingdom, according to news reports there were damaged infrastructures in Fès, Errachidia and Nador. From the 23d till the 26th, torrential rain hit the far North East of the country and more precisely, the Mediterranean coast line, the Rif and the Mid-Atlas. Over 24 hours, total rainfall over Tanger reached 200mm, 129mm in Alhoceima, 123mm in Nador and 94mm in Tétouan.

The aim of this study is to evaluate simulated θ from large to mesoscale models over the heavily stormy period from the 9th to the 28th of October 2008 over Morocco. The first part will deal with an analysis of the severe meteorological event of the 23d of October 2008. the ensuing parts will deal with the evaluation of models (ECMWF 20km, ALBACHIR oper 16,7km, ALBACHIR 10km and AROME 2,5km) in regards to observations.

5.3.2. Weather context and analysis of the 23d October 2008 event

In Morocco, the inter-season (September-October) is usually characterized by the presence of hot air in the low layers of the atmosphere. Cold air from the North retreats back to the 40th parallel (to the North of France) leaving room for tropical jets to bring up warm air to the country. Meteorological conditions in altitude are often marked by dominating anticyclonic ridges. But from time to time, some small cold outbreaks can get through from the North Atlantic. The mixing of low level hot air and higher level cold air triggers the instability especially over mountainous areas.

In the lower layers, hot weather lasted the whole of August 2008. Many cold outbreaks were associated with deep thalwegs with low geopotential values. The strong instability and stormy systems were fostered by these two key factors. The synoptic analysis of the 23d of October 2008 reveals that the high-level thalweg was very deep and that the temperature of the cold outbreak air masses was very low. In the Mediterranean region, East and North East onshore winds amplified the instability by carrying an important flux of humidity inland. Thus, the Tangier region was hit by severe thunderstorms. This very serious meteorological situation was confirmed by satellite pictures where the convective cell that caused flooding in Tangier is clearly visible. Furthermore, the hourly precipitation diagram from Tangier harbour shows the timing of rain during the “black Thursday” of the 23d of October. The maximum fell between 1 et 7 PM with a climax between 3 and 4 PM lasting about 45 minutes.

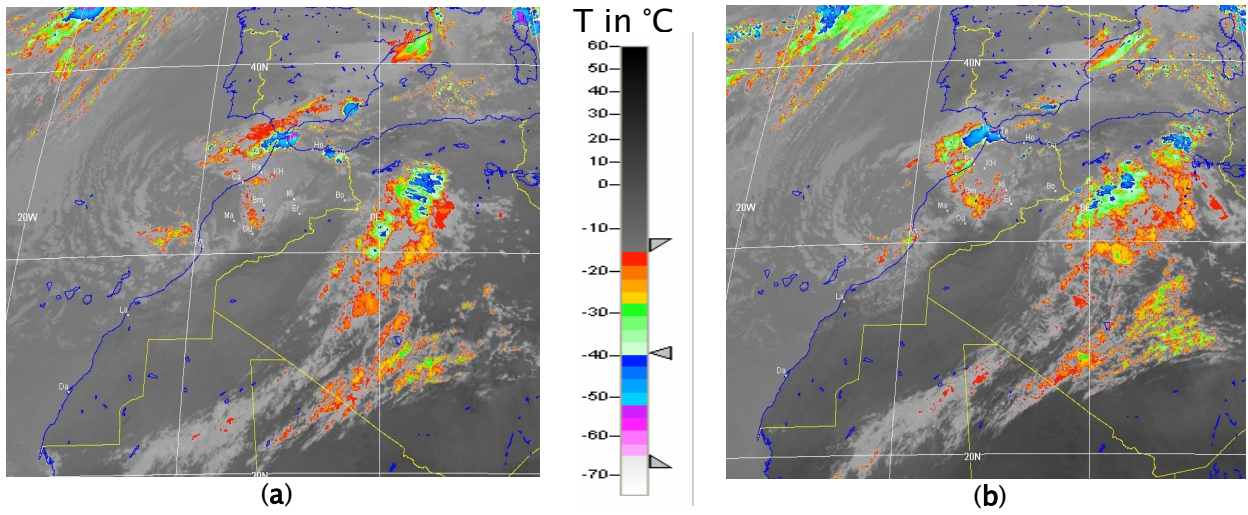


Fig 2: Infra red satellite images (10.8µm canal) the 23d October 2008 at 10 AM (a) and at 2 PM (b).

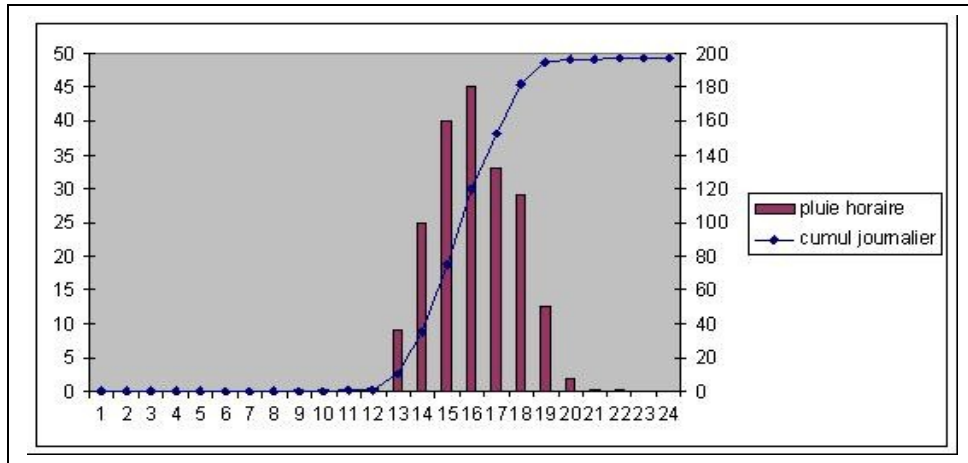


Fig.2: Hourly rainfall for Thursday 23d from Tangier harbour

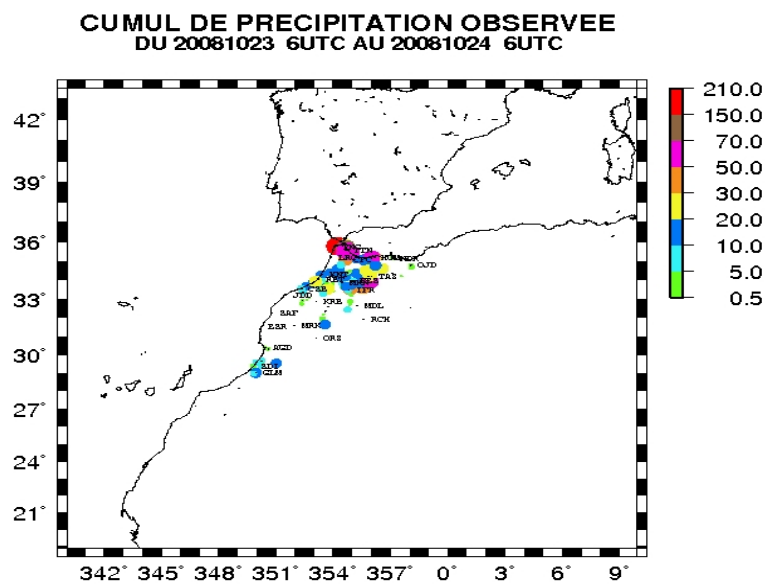


Fig.3: Total amount of observed precipitation in mm in 24h

5.3.3. Behaviour of the operational ALBACHIR model

In meteorology, the notion of space and time-scale plays a key role. As a matter of fact, the scale of meteorological events varies from a few hundreds or thousand kilometres (perturbations, frontal systems that may last several days) to several kilometres (isolated storm that lasts a few hours or even less). Large scale phenomena are well taken into account by numerical models, but small scale ones, because of their size and duration, are more difficult to comprehend.

The DMN operational numerical model (operational ALBACHIR 16,7 km for CY29t2) has simulated quite accurately the meteorological event of October 2008. Instability indices such as low level heat fluxes and the presence of upper level minima have been well predicted . However, the model was unable to pinpoint storms and their intensity. (Fig.5)

For the particular case of the 23d of October, fig.4a shows that the altitude (height) minimum was deeper and that upper level temperature was very low. The field of vertical velocity forecasted for 18h by operational ALBACHIR (fig.4b) shows, but shifted in time and space the areas where the instability as well as the vertical extension of clouds were very important.

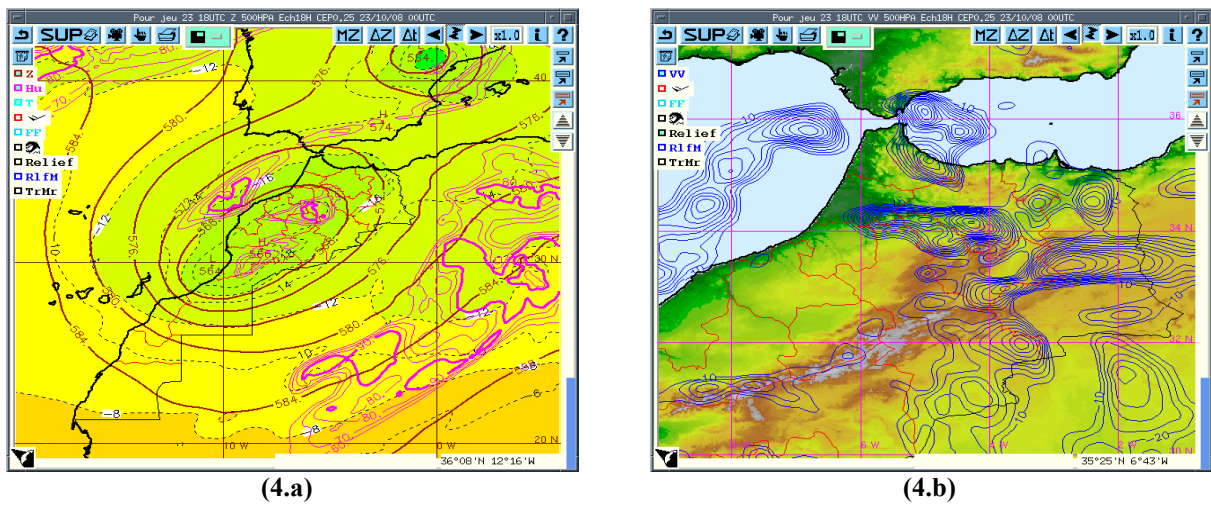


Fig.4: Operational ALBACHIR geopotential and temperature (a) vertical speed field (b) at 18h

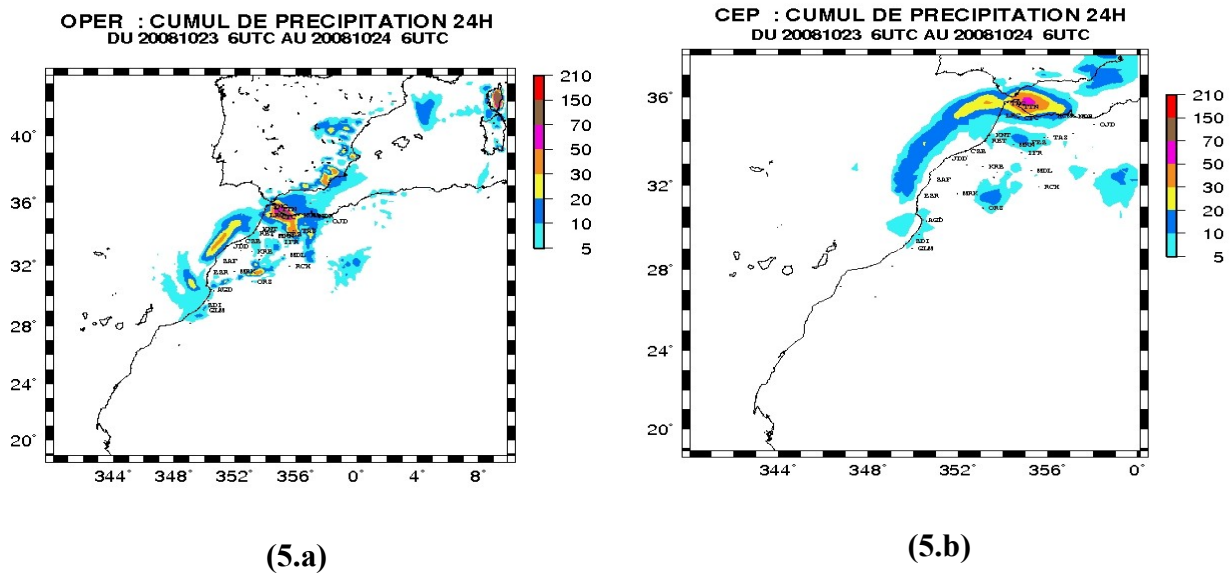


Fig.5: 24h total amount of precipitation predicted by ALBACHIR (a) and ECMWF (b)

5.3.4. Forecasted precipitation by ALBACHIR 10km for the 23/10/2008

The difficulties encountered by operational ALBACHIR to spot the convective systems of the 23d of October 2008, led us to test a new configuration based on the latest CY33t0 with a 10 km resolution.

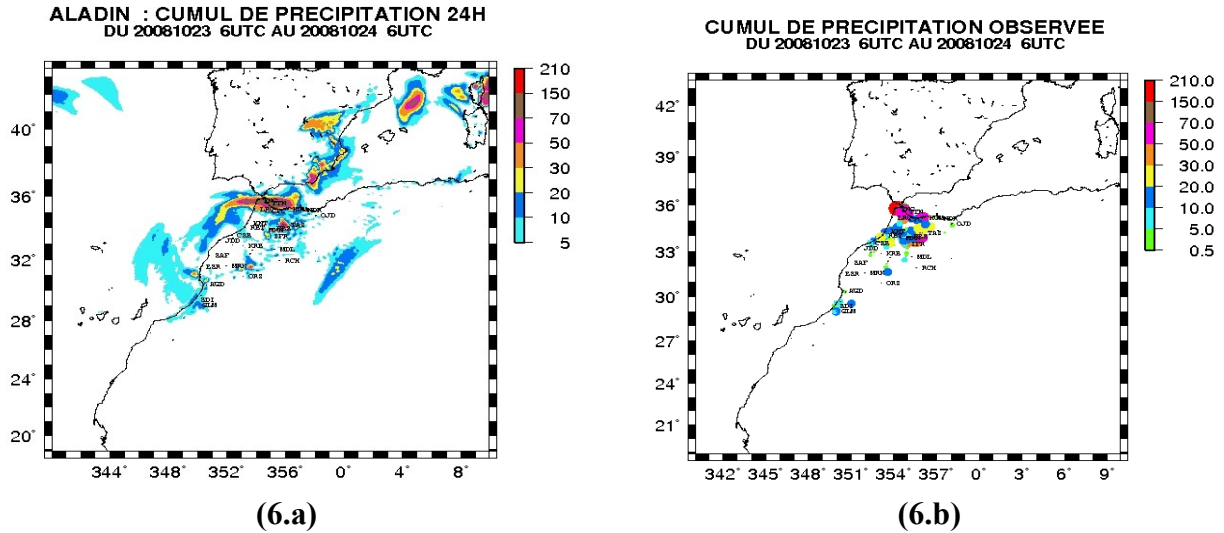


Fig.6: 24h total precipitation predicted by ALBACHIR (10 Km) for the 23/10/2008 (a) and observations (b)

The latest version of the ALBACHIR model (CY33t0) with its 10km grid has enabled to slightly ameliorate the precipitating structures of the 23d of October 2008.

5.3.5. The very high resolution model AROME

The Cloud Resolving Model AROME¹ was used during the whole month of October for daily forecasts with a 24 hour range. The initial conditions come from an interpolation of ALBACHIR outputs (10km) on the AROME grid (2.5km). All experiments use CY33t0, the operational model uses CY29t2.

Figure 7 shows that AROME predicts a maximum total rainfall of 200mm per 24 h, which is what the observations show as well as the recorded flooding in the North of the country. But these maxima were localised near the South East of Tangier and were far more widespread on other areas.

For a rigorous validation of the precipitation field, 24h forecast were launched with the three models for the month of October. Then, statistical parameters were computed to get the following scores: bias, ACC (forecast ACCuracy), POD (Probability Of Detection), FAR (False Alarm Rate) and ETS (Equitable Threat Score).

¹ AROME 2.5 km uses the non hydrostatic dynamics of the ALBACHIR model as well as meso-NH physics. Its forecasts at 24h. At this resolution, the deep convection est supposed explicitly resolved. From the ALBACHIR (10km) analysis at 00 UTC, it is coupled with the forecast every three hours.

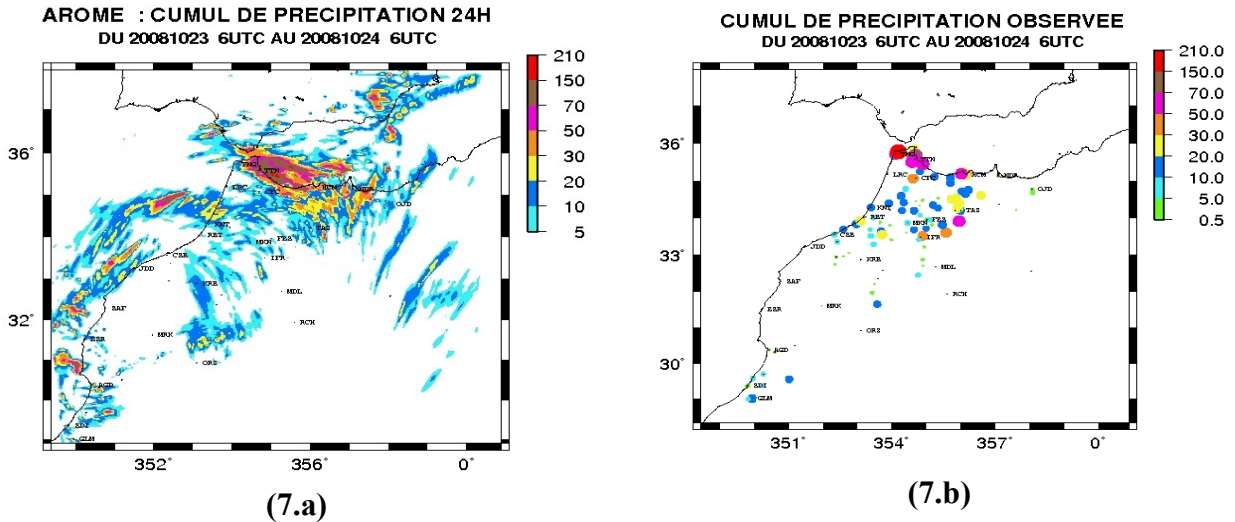


Fig.7: 24h total amount of precipitation for the 23/10/2008 from AROME 2.5km (a) and observations (b)

5.3.6. Evaluation of simulated rainfall against observations

The evaluation of predicted rainfall by the ECMWF (20km), ALBACHIR (16.7km), ALBACHIR (10km) and AROME (2.5km) models against observations can be made either by comparing the two rainfall charts or more rigorously (objective evaluation) using statistical diagnostics.

Because precipitations are not continuous, the objective evaluation can be made using categorical contingency tables. These tables give the frequency of predicted or observed precipitations below or above a predetermined threshold R.

		Predicted	
		rain<R	rain>R
Observed	rain<R	a (good predicted)	b (false alarm)
	rain>R	c (note detected)	d (good predicted)

For each of the four models, to compute bias, ETS, FAR, POD and ACC scores, first of all, we made an interpolation of predicted rainfall at the observation point (Cressman interpolation). The thresholds used for the computation of the different scores are as follow: 0.2, 1, 2, 5, 10, 20, 30 and 50 mm. The mathematical formulae for the computation of the scores can be found in Hdidou F.Z.'s paper: "Validation des précipitations ALADIN par rapport aux precipitation CPC (Climate Prediction Center, NOAA)".

□ Accuracy rate (ACC)

The accuracy rate (ACC) is defined as the ratio between correct forecasts (occurrence or non occurrence of events) and the total number of forecasts. Non precipitating events are predominant, the ACC index is much influenced by these non-events which therefore may induce in misleading information about the quality of the forecast, especially in dry areas.

In fig.8a, one can see that the accuracy rate is above 0.75 for all thresholds which means that the rainfall forecast is good. It must be noted that for heavy rainfall (>20mm/24H), the accuracy rate is very close to 1. However, if one compares indexes a and d from the contingency table, it appears

that d is insignificant before a , therefore “heavy rainfall” cells are not well located by the model.

□ **Probability of detection (POD)**

The probability of detection measures the ability of a prediction system to well predict precipitating events ($\text{rain} > T$).

Fig 8b shows the probability of detection computed for the precipitations of the four models (ALBACHIR OPER, ALBACHIR 10km, AROME 2.5km and ECMWF) from the 8th till the 29th of October 2008. One can see that the four models predict rather well precipitation less than 10mm with a lesser probability for AROME. There is a positive bias in the prediction of surface temperatures that tends to dry out light precipitation in the lower layers (which is a known problem of AROME). But, no model accurately predicts strong precipitation ($>20\text{mm}/24\text{h}$).

To be noted the slight improvement of ALBACHIR 10km and AROME 2.5km for heavy rainfall against operational ALBACHIR (OPER).

□ **False Alarm Rate (FAR)**

The False Alarm Rate is the ratio of false alarms with respect to the predicted number of events. From figure 8c showing the FAR for precipitations for the four models, one can see that one gets many more false alarms for heavy precipitations than for light ones ($< 10\text{mm}$).

ALBACHIR 10km and AROME 2.5 km improve the prediction of heavy precipitations by lowering the false alarm rate for $\text{RR} > 50\text{mm}$, which is not the case for the other operational models.

□ **ETS**

ETS measures the degree of coincidence of forecasts against observations, taking into account fortunate good forecasts. More often than not it is used to check deterministic forecast of rare events such as severe precipitations. Its values ranges from 1 for a perfect forecast to 0. An ETS of 0,5 is considered good, exceedingly good for 0,6. this measure is quite interesting as it is not as much influenced by the “no precipitation event” as ACC is.

From figure 8d, one can see that the value of the ETS equals 0.4 for a threshold of 0.2 and it increases for thresholds of 1 and 2 mm, it decreases at other thresholds, which is an indication that models do distinguish rain from no rain but err as to the localisation of heavy rain. ALBACHIR 10km and AROME score better for heavy precipitations.

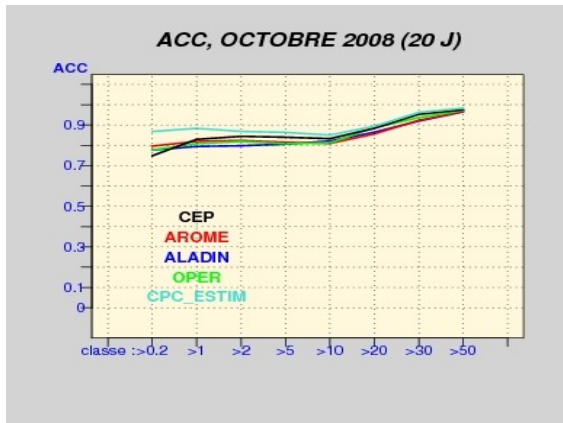
□ **Bias**

The bias is the ratio between the number of forecasts and the number of observations of a given event. In our case, the event is the number of precipitation above the threshold T . Biases vary from 0 to infinity. If the bias is less than 1 ($\text{bias} < 1$), predicted precipitations are underestimated, but if it is greater than 1 ($\text{bias} > 1$) predicted precipitations are overestimated.

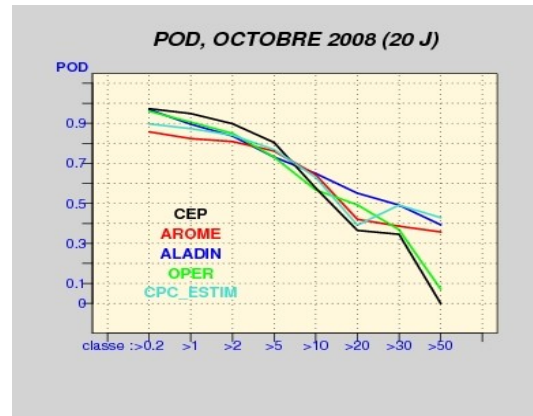
Figure 8e shows the computed bias for ALBACHIR 10km, AROME, ECMWF and ALBACHIR operational precipitations and the predictions from the Climate Prediction Center (CPC) for October 2008 (20 days). First of all, CPC underestimates precipitations above 5 mm, but this model does not take into account the orography.

ALBACHIR 10km, ALBACHIR OPER and ECMWF slightly overestimate precipitation less than 10mm. AROME has a bias close to 1 for precipitation rates less than 20mm.

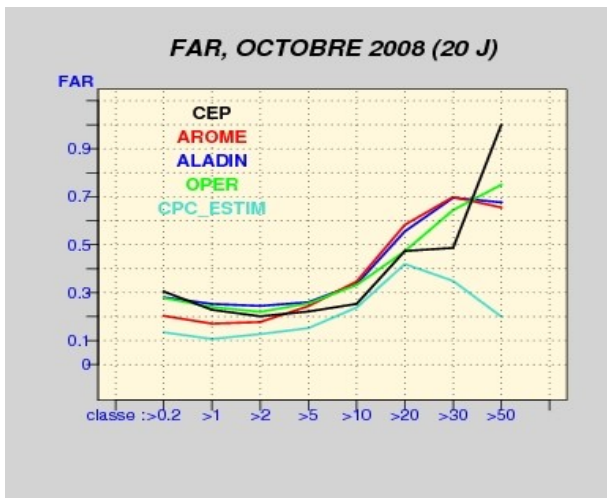
ALBACHIR 10km and AROME overestimate whereas ALBACHIR OPER and ECMWF underestimate heavy precipitations ($>30\text{mm}$).



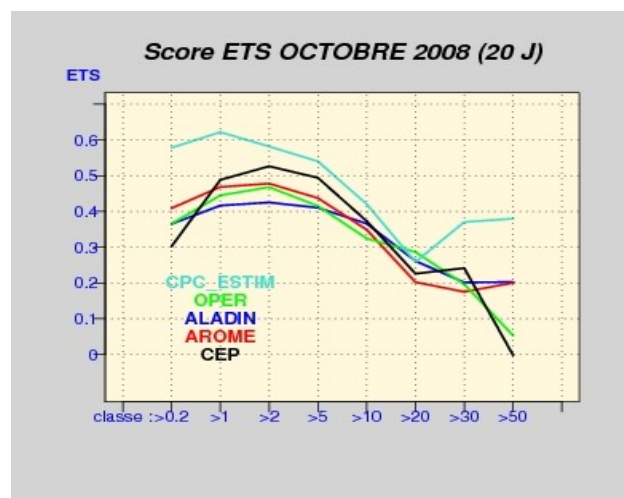
(8.a)



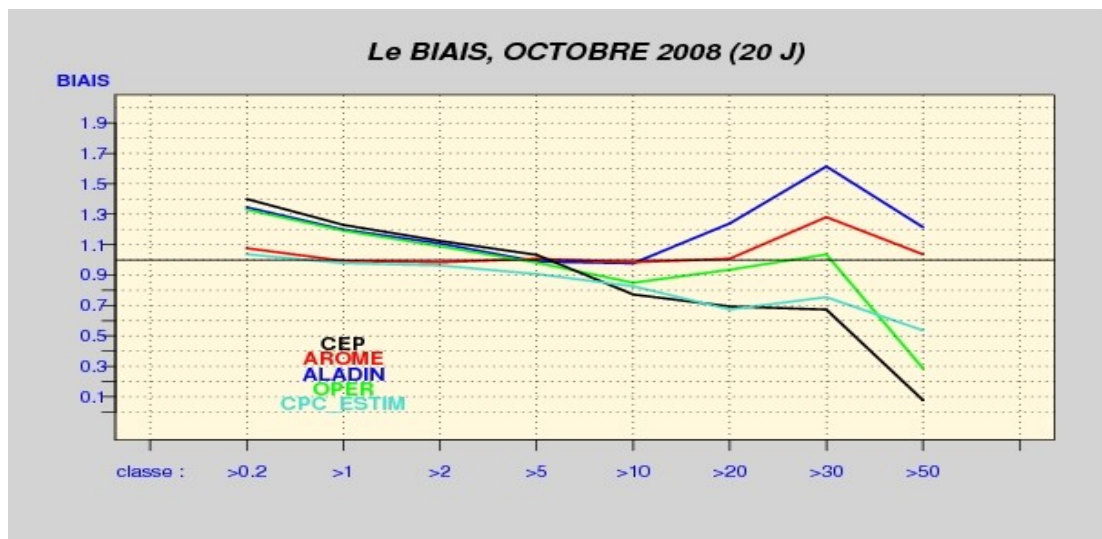
(8.b)



(8.c)



(8.d)



(e)

Fig 8 : ETS, FAR, POD, ACC and Bias scores for October 2008

5.3.7. Conclusion and future prospects

The October 2008 precipitations were exceptional for Morocco. Records were broken and surpluses over 1000% with regard to the norm (over a 30 year period) were recorded in some areas.

From a dynamical point of view, the numerical model operating at DMN (ALBACHIR 16.7 km/ CY29t2) predicted rather well the meteorological events of October 2008 (the large scale instability indexes were well predicted). However, the model was at fault as to localise the storms and to gauge their intensity.

The latest version of the ALBACHIR model (CY33t0) with its 10km grid has enabled to slightly ameliorate the precipitating structures of the 23d of October 2008.

The maximum precipitations predicted by AROME 2.5km are confirmed by observations and also by the flooding of the North of the country. But these maxima were inaccurate as to the time and their number was overestimated..

Computed scores for the period 8-29 October 2008 have shown that ALBACHIR OPER and ECMWF models tend to underestimate heavy precipitations whereas ALBACHIR 10km and AROME overestimate them. The latest 10km grid ALBACHIR version bettered the prediction of the heavy precipitations that occurred during the month of October 2008 over Morocco.

The precipitation data used in this study come from the synoptic network supervised by the Centre National d'Exploitation Météorologique. However, most of these data come from ancillary stations not supervised by CNEM. The conclusions are very much dependant on the quality of data used in the study.

AROME seems to have great potential to correctly predict severe events. The dynamic adaptation shows some limits for this type of model and the variational assimilation is a must for predicting for high resolution events. The benefits of meso scale data assimilation (grid < 10km) should be felt for local events, linked to convection and/or orography, such as low layers convergence fluxes, cooling under storms or at the bottom of valleys. Firstly, meso-scale models can simulate these events/phenomena, but on top of that, the analysis can take into account and accept observations such as surface data.

In France, radar data assimilation experiments (reflectivity and radial velocity) have slightly bettered the localisation of convective cells. With the acquisition of meteorological radars by Morocco, SPN can hope for a similar development for AROME NORD MAROC experiments.

The initial surface conditions are of prime importance for AROME. Surface files used in our experiment have a coarse resolution over Morocco (towns badly represented, incomplete soil texture...), these data are used in several surface schemes (towns, lakes ...). Efforts must be sustained so as to create good quality data bases.

References :

- ALADIN Numerical Weather Prediction Project web pages : <http://www.cnrm.meteo.fr/aladin/>
- K.LAHLAL, La situation météorologique des mois de Septembre et octobre 2008 sur le Maroc.
- F.Z.HDIDDOU, validation des précipitations ALADIN par rapport aux précipitations CPC, 2007.

Acknowledgement:

The author wishes to thank J-A Maziejewski for translating this paper.

5.4. Ensemble background-error variances: Objectives Filtering and Impact Studies.

Raynaud L.

Background-error variances are key components to any data assimilation scheme, since they determine the respective weights of the background and of the observations in the analysed state.

Partly related to the work of Evensen (1994) on the Ensemble Kalman Filter (EnKF), the use of an ensemble of assimilations (Houtekamer et al., 1996; Fisher 2003; Belo Perrera and Berre, 2006) to estimate background-error covariances has been widely tested in the recent years. This attractive method offers the possibility to calculate covariances of the day in a data assimilation system, and also to understand the spatio-temporal dynamics of these statistics. Therefore, this is a particularly relevant framework for background-error covariance modelling.

However, random errors in the variance estimation arise from the finite ensemble size, through the associated sampling noise. When planning to use such ensemble-based estimates in a data assimilation scheme, some filtering tools must then be implemented.

Regarding filtering procedures, a first empirical study by Raynaud et al. (2008) showed that an optimized local spatial average of the variance field should help to calculate accurate estimates. However, the tuning of this optimal averaging is not so obvious, all the more so because it is likely to vary with both vertical level and background-error length-scale. Thus, it can represent a large amount of work in an operational setting.

An objective and automatic spectral filtering technique has then been proposed by Raynaud et al. (2009). The analytical formulation relies on an estimate of noise-to-signal ratios. This results in a low-pass filter according to the relative contributions of signal and noise.

The application of this filter to the error variances derived from the Arpège ensemble assimilation shows that the filter is robust and relevant. One interesting feature is that it is able to adapt to the vertical level and to the parameter considered. More precisely, the truncation of the filter decreases with altitude, which results in a rather light filtering at lower levels while it is much more stronger at upper levels. The filter also preserves the largest scales which are relatively well-sampled spatially.

Figure 1 shows both raw and filtered maps of vorticity standard deviation near the surface and in the mid-troposphere. Raw maps are clearly affected by sampling noise. When looking at the corresponding filtered maps, one can see that the filtering succeeds in removing most of the sampling noise while preserving the signal of interest. Filtered maps reach a level of accuracy of around 10%.

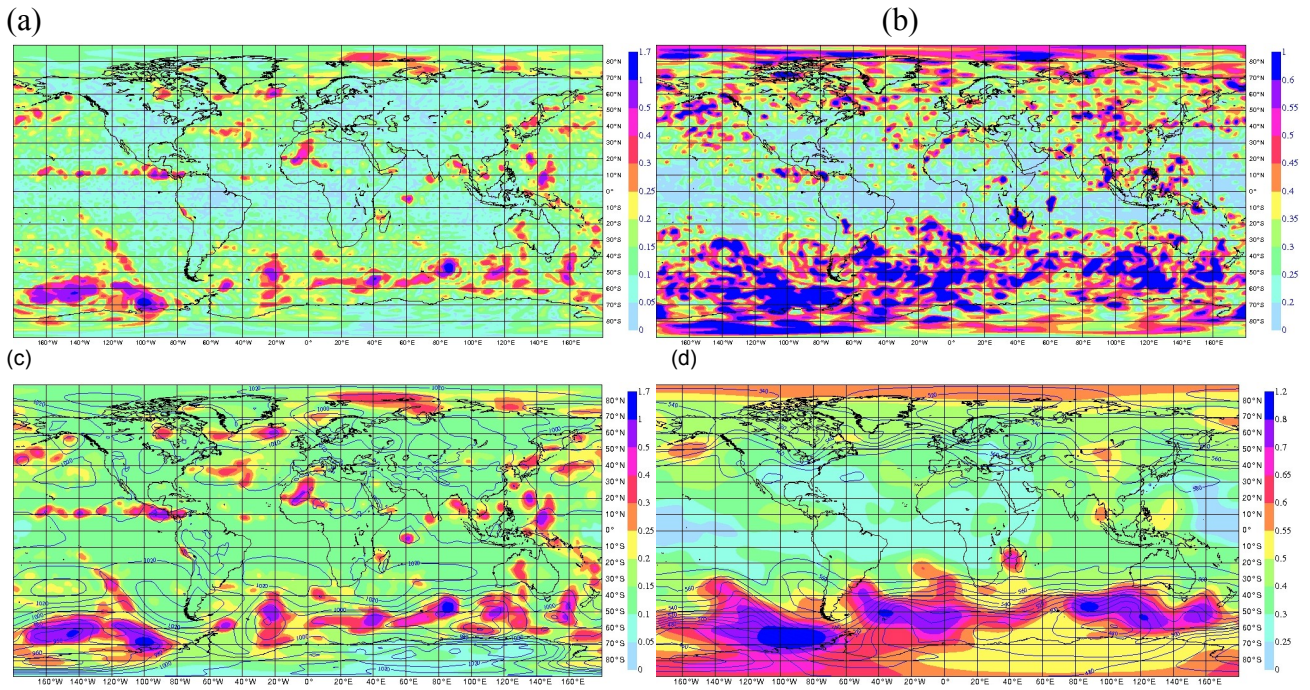


Fig 1. Standard deviation maps of vorticity ($5 \times 10^{-5} \text{s}^{-1}$) at 00 UTC on 15 September 2007. (a)-(b) Raw maps near the surface and at 500hPa. (c)-(d) Corresponding filtered maps.

This filtering procedure provides smooth and accurate variance maps, however, it is worth examining if it has a real impact on the assimilation and forecast systems in the end. Two impact studies over a February-March 2008 period showed that the use of the filter helps to increase the background fit to the observations on the one hand, and to provide more accurate forecasts on the other hand.

Finally, evaluating the gain from using variances of the day instead of climatological variances is another important aspect. A number of impact studies performed with the Arpège assimilation system show that a positive global impact is obtained, especially from the use of flow-dependent humidity variances. But the highest improvement is observed locally on extreme weather events. Figure 2 shows two 48h-forecasts of surface pressure for the severe storm that hit the Northern part of France on 10 February 2009. The first forecast (in blue) uses climatological variances for all control variables, while the second forecast (in red) uses variances of the day for all control variables. Compared to the analysis, the climatological σ^b run is relatively inaccurate since the center of the storm is moved to the south-west. When variances of the day are used, this position error is significantly reduced (and the intensity error too). Further studies show that this great improvement can be in large part attributed to the use of flow-dependent surface pressure variances.

As a conclusion, impact studies show that there is a rich and robust information in the flow-dependent variances derived from the ensemble assimilation. This information can be emphasized thanks to the objective filtering, which helps to only retain the relevant scales in the variance maps (while filtering out the noisy ones). This flow-dependent information may be particularly relevant for the prediction of intense weather events.

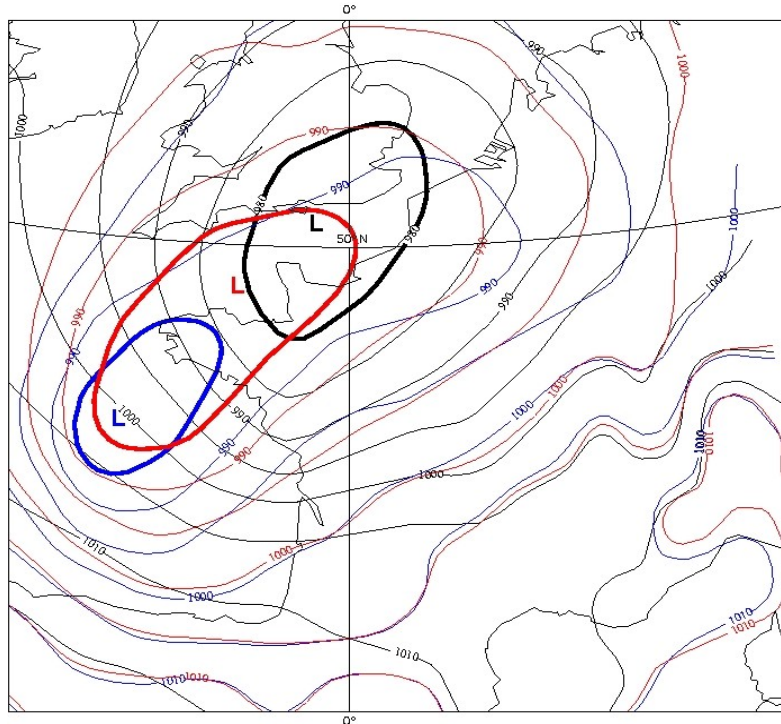


Fig 2. 48h Arpège forecasts of surface pressure valid on 10 February 2009 at 00 UTC. In blue (resp. In red), the forecast issued from an assimilation using only climatological (resp. flow-dependent) variances. The reference analysis is shown in black. Contour : 5hPa.

Reference

Belo Pereira, M., and L. Berre, 2006 : The use of an ensemble approach to study the background error covariances in a global NWP model. *Monthly Weather Review*, 134, 2466–2489.

Berre, L., O. Pannekoucke, G. Desroziers, S. E. Stefanescu, B. Chapnik, and L. Raynaud, 2007 : A variational assimilation ensemble and the spatial filtering of its error covariances : increase of sample size by local spatial averaging. *Proceedings of the ECMWF Workshop on Flow-dependent aspects of data assimilation*, 11-13 June 2007, pages 151–168. Available on line at :

<http://www.ecmwf.int/publications/library/do/references/list/14092007>.

Fisher, M., 2003 : Background error covariance modelling. *Proceedings of the ECMWF seminar on recent developments in data assimilation for atmosphere and ocean*, ECMWF, pages 45–63.

Evensen, G., 1994 : Sequential data assimilation with a nonlinear quasigeostrophic model using monte carlo methods to forecast error. *J. Geophys. Res.*, 99, 10143–10162.

Houtekamer, P. L., L. Lefaivre, J. Derome, H. Ritchie, and H. L. Mitchell, 1996 : A system simulation approach to ensemble prediction. *Monthly Weather Review*, 124, 1225–1242.

Raynaud, L., L. Berre, and G. Desroziers, 2008 : Spatial averaging of ensemble-based background-error variances. *Quart. J. Roy. Meteor. Soc.*, 134, 1003–1014.

5.5. Monitoring the coupling update frequency on the LACE coupling domain

Tudor Martina

Summary

Analysis of the MCUF (Monitoring of the update frequency) field has been performed for the LACE coupling domain for the period since 23rd January 2006, when it became available.

5.5.1. Introduction

Termonia (2003) has analysed the Lothar storm (Wernly et al. 2002) and found that the three hourly coupling update interval is insufficient for resolving the storm in lateral boundaries. This lead to a solution proposed in Termonia (2004) where a strategy of monitoring the coupling update frequency has been proposed. This lead to production of the so called MCUF field in the output of ARPEGE and provided in the coupling files since 06 UTC run on 23rd January 2006 for the common LACE coupling domain. When this field is larger than some threshold value, there is a rapid “development” in the surface pressure suggesting that a fast cyclone has moved through the area. If the point with the large MCUF value is inside the coupling zone of the ALADIN model domain, it can be expected that the ALADIN model run will miss the cyclone strength and development due to time interpolation of boundary data.

When the time series of these data has been analysed for the Belgian domain (Termonia et. al. 2009), it was found that such events occurred only several times per year and they proposed to restart the model forecast from the coupling file when the storm is inside the domain using the scale selective digital filter initialization (Termonia, 2008).

This article will present the analysis of the MCUF field for the common LACE coupling domain.

5.5.2. Time series of the MCUF maxima

The maximum value of the MCUF field has been extracted from each coupling file available, for 4 runs per day (starting from 00, 06, 12 and 18 UTC analyses) and extending 72 for the first 3 or 60 hours for the 18 UTC run.

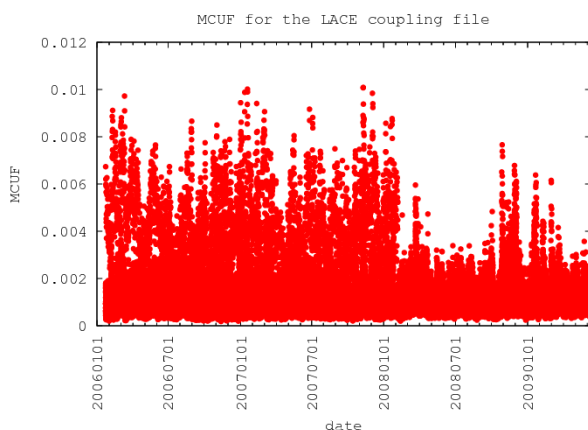


Fig.1: Time series of maximum value of MCUF on the LACE domain for all forecast coupling files.

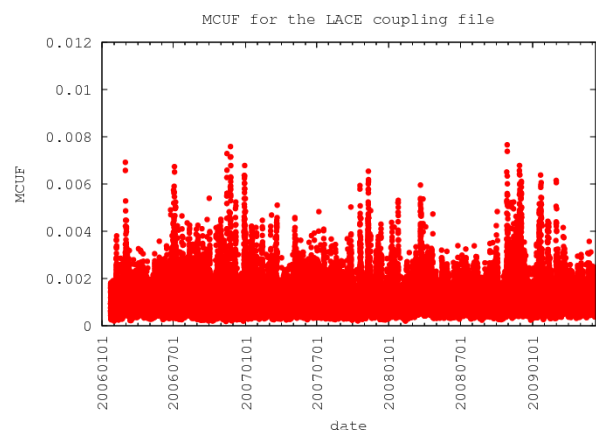


Fig.2: Time series of maximum value of MCUF on the LACE domain for forecasts ≥ 6 hours.

Figure 1 shows the values of the MCUF maxima for the whole domain. It can be seen that the value of 0.003 has been exceeded very often until 06 UTC run on 6th February 2008. However gross number of these large values is from the +03 hour forecast coupling files. This suggests large spin-

up of the surface pressure field in the beginning of the ARPEGE forecast. Changes in the data assimilation (initialization) of ARPEGE introduced in the 06 UTC run on 6th February 2008 removed this spin-up. Since these large values of MCUF in the +03 hour forecast mostly do not represent a storm that moves quickly through the domain, analysis has been performed only on fields from +06 hour forecast or larger. The number of cases reduced significantly (Figure 2).

This date also corresponds to a change in resolution of the coupling files, from 20.675 to 15.4 km. Most of the points with large MCUF values in the 3 hour ARPEGE forecast are close to mountains (Figure 3).

Spatial distribution of MCUF>0.003 for the LACE coupling domain

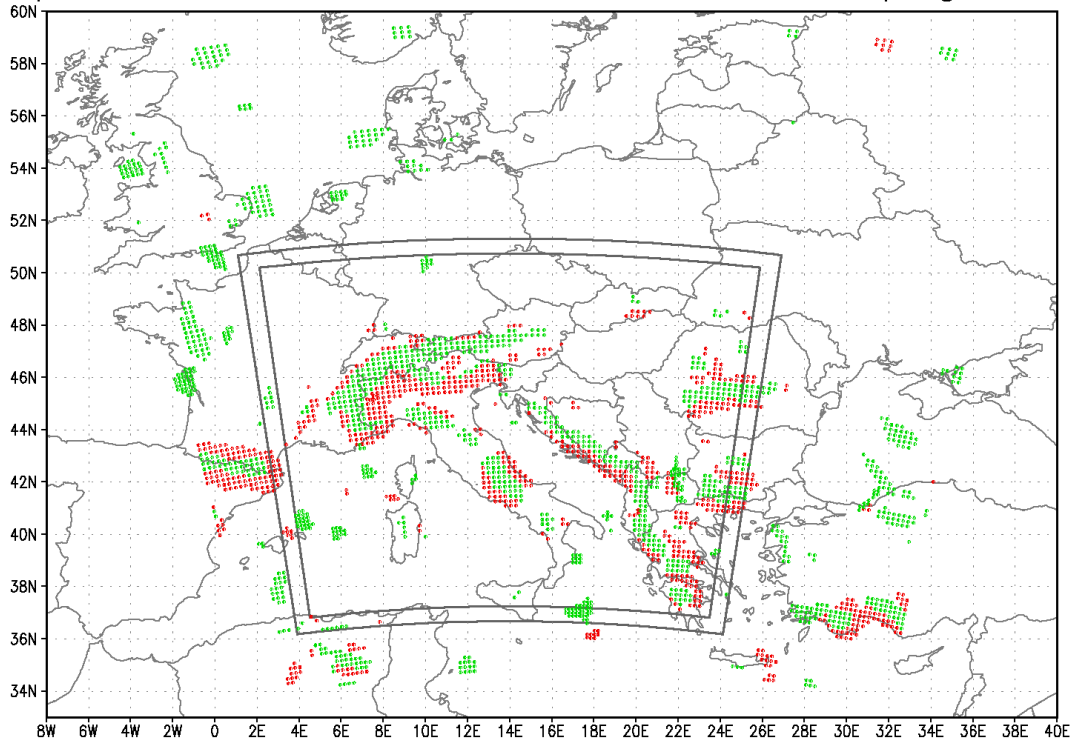


Figure 3: Spatial distribution of the large MCUF values for MCUF > 0.003 and 03 hour forecast only. The coupling zone of the operational ALADIN-Croatia domain is also shown.

5.5.3. Spatial distribution of the large MCUF values

All points where the absolute value of the MCUF field has been larger than the 0.003 threshold have been extracted from all the coupling files where the field was available. When these points are plotted on a map (Figure 3), it can be seen which areas should be avoided as parts of the coupling zone if one wants to have less problems with properly resolving the boundary data.

It can be seen that the storms move rather quickly from Atlantic (west and north west side of the domain) or over North, Baltic and Mediterranean seas.

Each case with MCUF > 0.003 has been analysed and several cases when the cyclone entered the domain will be presented. The goal is to find a case when one storm quickly enters the domain, while another one is already present in the domain area.

Spatial distribution of $MCUF > 0.003$ for the LACE coupling domain

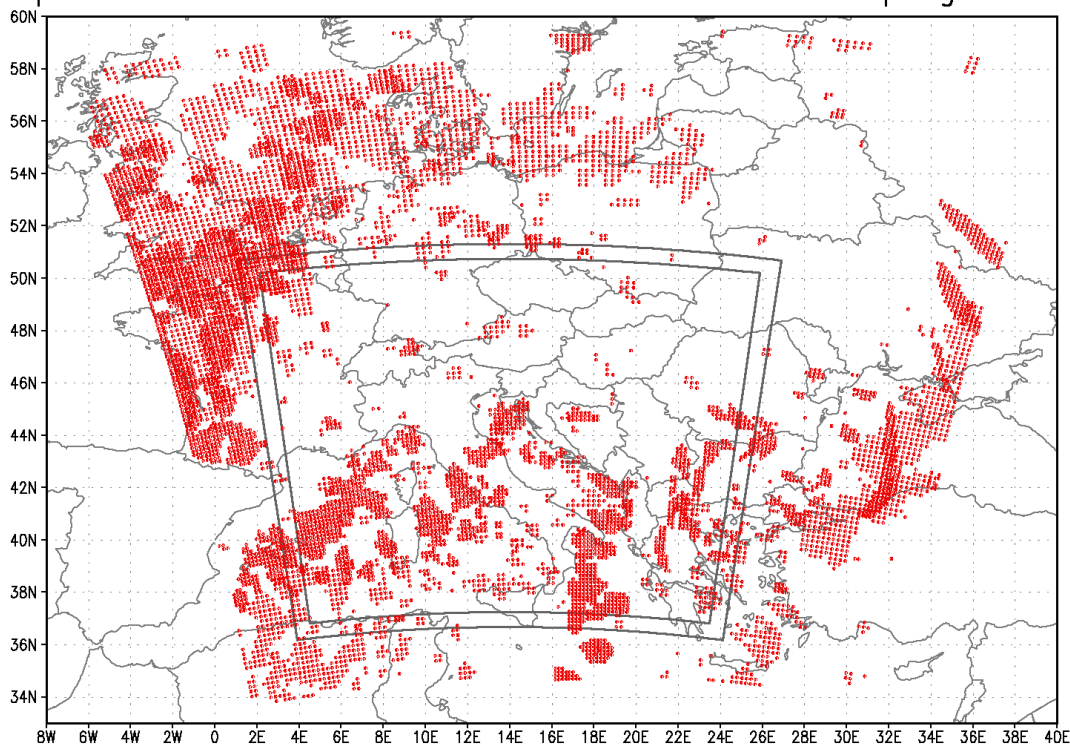


Figure 4: Spatial distribution of the large MCUF values for $MCUF > 0.003$ and forecast hour ≥ 06 hours. The coupling zone of the operational ALADIN-Croatia domain is also shown.

5.5.4. Several interesting cases

The total number of cases when the critical value of MCUF was exceeded in the period from 06 UTC run on 23rd January 2006 until 21st July 2009 in any coupling file for at least 6 hour forecast is 1161 (analyses and 3 hour forecasts were omitted from the count). This number refers to the whole LACE coupling domain and only a small portion of that number refers to cases when the MCUF value is exceeded in the coupling zone of the ALADIN Croatia domain. Figures were plotted of the mean sea level pressure gained by fullpos of the coupling file and the points where the critical value of MCUF has been exceeded only for the 00 and 12 UTC runs.

The author did not make a detailed classification of the cases (incoming and outgoing cyclones and fronts and those completely inside or outside the domain) but apparently, the operational ALADIN Croatia domain is very fortunately situated, as can be seen even in Figure 4, most of the cyclones either pass north of the domain barely touching its edge, or develop inside, only those that arrive from the western Mediterranean Sea or from south enter the domain too quickly to be properly represented on the boundary using 3 hourly data.

Several cases relevant for the operational ALADIN Croatia domain are presented in Figures 5 to 8.

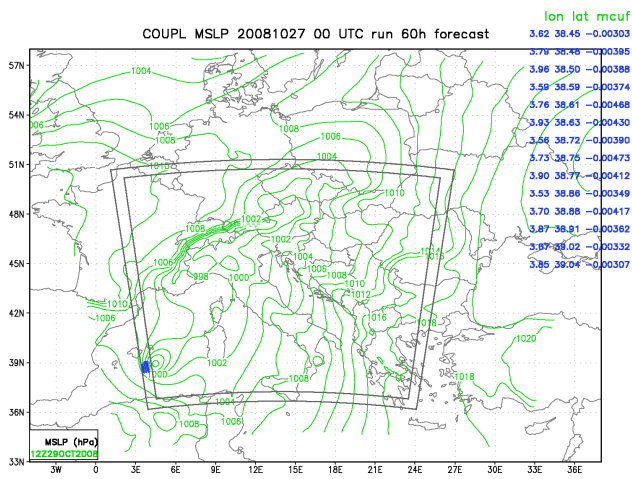


Figure 5: Storm entering the domain from the west, 60 hour forecast starting at 00 UTC 17th October 2008. Fields from 57 hour forecast starting at 12 UTC the same day and 33 and 12 hour forecasts from 00 UTC analyses of 28th and 29th October 2008 give similar results.

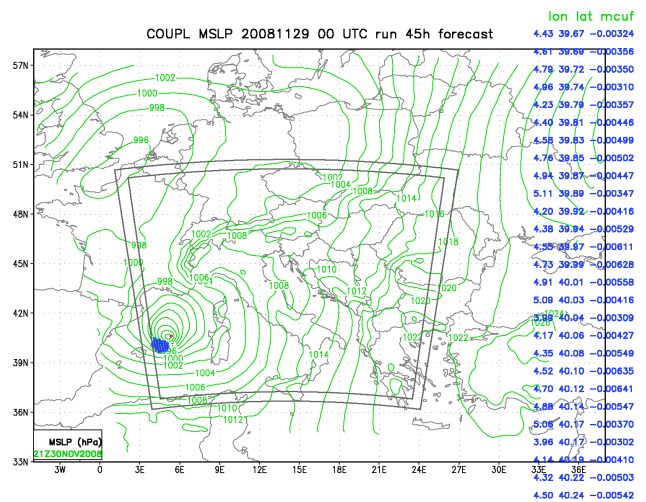


Figure 6: Storm entering the domain from the west, 45 hour forecast starting at 00 UTC 129th November 2008. Fields from 57 hour forecast starting at 12 UTC the previous day and 33 and 18 hour forecasts from 12 UTC on 29th and 00 UTC on 30th November 2008 give similar results.

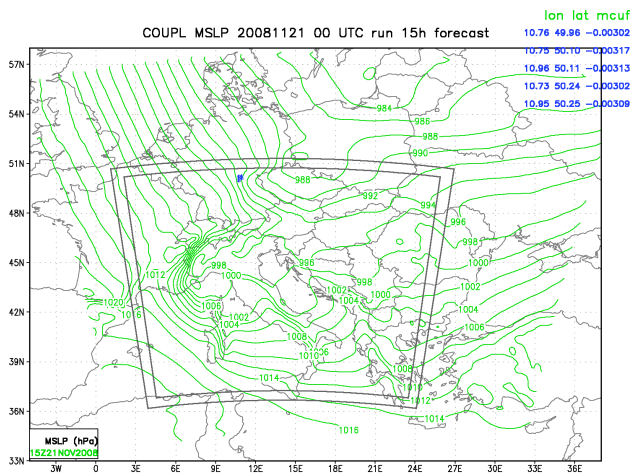


Figure 7: Front entering the domain from the north, 15 hour forecast starting at 00 UTC 21st November 2008. The existence of Genoa cyclone in the domain makes this case interesting for further study.

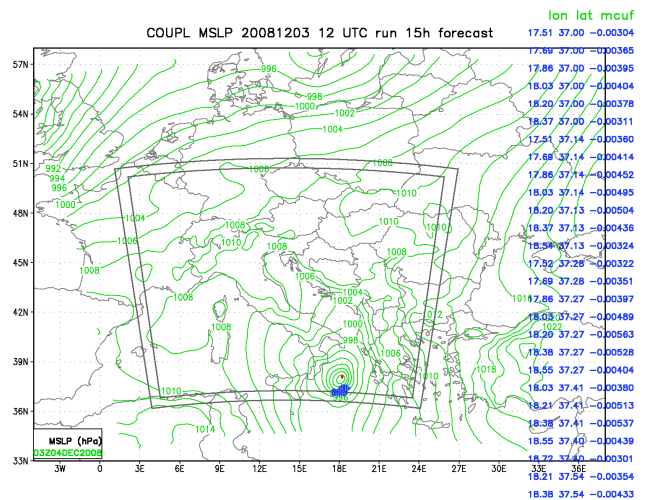


Figure 8: Storm entering the domain from the south, 15 hour forecast starting at 12 UTC 3rd December 2008. Fields from 27 hour forecast starting at 00 UTC the same day, 54 hour forecast of the 00 UTC run of the previous day and 66 hour forecast from 12 UTC 1st December 2008 give similar results.

5.5.5. Conclusions

Analysis of the MCUF field for a longer period can show which areas favour quickly moving storms that could be missed by the coupling procedure if the 3 hourly coupling period is used. Depending on the choice of the domain, the number of cases when the critical MCUF value is exceeded may vary significantly.

The work presented here was accomplished by a semi-automated procedure that finds the maximum MCUF value in each file and prints it out in an ASCII file containing its value and coordinates. It is also possible to use the same procedure and printout all points where the MCUF value is larger than some prescribed threshold. Anyone wishing to repeat the work for some other domain can port it home and use it at will.